

Sound Methods of Breaking Foam

Fourth Year Project Report- Engineering Science, Finals Part II, 2007

James Winterburn, Pembroke College

Supervised by Dr P. Martin



**FINAL HONOUR SCHOOL OF
ENGINEERING SCIENCE**

DECLARATION OF AUTHORSHIP

You should complete this certificate. It should be bound into your fourth year project report, immediately after the title page. Three copies of the report should be submitted to the Chairman of Examiners for your Honour School, c/o Clerk of the Schools, Examination Schools, High Street, Oxford.

Name (in capitals): JAMES WINTERBURN

College (in capitals): PEMBROKE

Supervisor: DR P.MARTIN

Title of project (in capitals): SOUND METHODS OF BREAKING FOAM

Word count: 9571 (Including abstract)

Please tick to confirm the following:

I am aware of the University's disciplinary regulations concerning conduct in examinations and, in particular, of the regulations on plagiarism.

The project report I am submitting is entirely my own work except where otherwise indicated.

It has not been submitted, either wholly or substantially, for another Honour School or degree of this University, or for a degree at any other institution.

I have clearly signalled the presence of quoted or paraphrased material and referenced all sources.

I have acknowledged appropriately any assistance I have received in addition to that provided by my supervisor.

I have not sought assistance from any professional agency.

The project report does not exceed 10,000 words plus 40 pages of diagrams, photographs etc.

I agree to retain an electronic version of the work and to make it available on request from the Chair of Examiners should this be required in order to confirm my word count or to check for plagiarism.

Candidate's signature: Date:

Acknowledgements:

Thanks to my project supervisor Dr P. Martin for his knowledge and invaluable guidance throughout the project.

Thanks to Jamie Condliffe for his advice and also sharing transducer pressure calibrations.

Thanks to Richard Gaskell for information regarding transducer behaviour and electrical characterisation of resonance.

Thanks to the EPSRC for loan of the Kodak EM high-speed camera.

Abstract:

A comprehensive literature review and experimental investigation of foam-ultrasound interaction is presented. Detergent based foam was subjected to low power ultrasound at two frequencies, 27.72kHz and 40.00kHz, allowing for any frequency dependency to be observed. The effects of the two frequencies of ultrasound on foam height, liquid drainage and collapse behaviour were compared to experiments conducted without ultrasound. In the case of 40.00kHz ultrasound an increased liquid drainage rate was observed and, for the first time, a pronounced increase and subsequent peak in mean liquid holdup was measured experimentally. These observations are shown to be independent of the initial liquid holdup of the foam. Photographic images of 40.00kHz ultrasound induced foam collapse provide visual evidence of the increased rate of liquid drainage and the change in the nature of collapse when ultrasound is involved. Experimental observations are explained in terms of foam collapse mechanisms identified in the literature review, and it is concluded that front rupture dominates collapse for foam under the influence of ultrasound.

Contents:

1. Introduction	1
2. Foams	3
2.1 Background	3
2.2 Foam structure	3
2.3 Laplace equilibrium	5
2.4 Surface active agents (Surfactants)	6
2.5 Foam drainage and stability	7
3. Methods of Foam Breaking	10
3.1 Background	10
3.2 Physical foam breaking methods	10
3.3 Chemical defoaming methods	11
4. Ultrasound	12
4.1 Background	12
4.2 Piezoelectric effect	12
4.3 Transducers	14
4.4 Impedance boundaries	17
5. Foam-ultrasound Interaction	19
5.1 Coupling between foam and ultrasound	19
5.2 Mechanisms of film rupture and the influence of ultrasound	21
6. Experimental Technique	24
6.1 Ultrasound generation	24
6.2 Surfactant solution makeup	24
6.3 Method of foam formation and liquid drainage/foam height measurements	25
7. Results	27
7.1 Ultrasonic transducer calibrations	27
7.2 Cumulative liquid drainage	30
7.3 Liquid drainage rate	33
7.4 Foam height	37
7.5 Variation of mean liquid holdup during foam collapse	40
7.6 Images of foam collapse	42
7.7. Foam fraction and ultrasonic foam breaker integration	44
7.8 Experimental errors and reproducibility	45
8. Discussion of Results	46
8.1 Rate of liquid drainage and cumulative global drainage	46
8.2 Mean liquid holdup	47
8.3 Foam collapse	47
9. Project Extensions	50
10. Conclusions	51
Appendix A. Progress report	53
Appendix B. Plastic cup design	56
Appendix C. Ultrasonic transducer pressure calibrations	57
Appendix D. Preliminary ultrasonic bath experiment results	60
Appendix E. Risk Assessment	61
Appendix F. COSHH Assessment	62
Appendix G. References	63

Nomenclature:

C	Capacitance (F)
D	Average bubble diameter (mm)
F	Frequency (Hz)
l	Displacement of crystal faces (mm)
L	Inductance (H)
dN	Rupture events in time interval dt
N	Total number of bubbles
P	Pressure (Pa)
q	Electrical charge (C)
r	Radius of curvature (mm)
R	Resistance (electrical) (Ω)
R	Reflection coefficient
t	Time (min)
T	Transmission coefficient
V	Voltage (V)

Greek Symbols:

a	Dimensionless liquid fraction
ξ	Dimensionless vertical position
ρ	Density (kgm^{-3})
τ	Dimensionless time
ω	Probability of rupture per unit time and unit surface

Subscripts:

b	Bubble
l	Lamella
pb	Plateau border
r	Resonant

1.Introduction:

Many practical situations arise in industry where the efficient destruction of foam is necessary. These foams can either be an undesirable by-product of a particular reaction or process, or an integral part of a specific unit operation. For instance nuisance foams can form in aerated vessels, such as chemostats used for the fermentation of sugars to alcohol using yeast (Perry and Green, 1984). Unwanted foam also occurs in the steam drum of industrial boilers, this foam must be carefully controlled to prevent priming of the boiler. Foam Fractionation is an example of a separation process that is used to purify surface active molecules, such as proteins, through adsorption to the liquid-gas interfaces in a foam, which is subsequently collapsed after liquid drainage has occurred, an enriched product being recovered (Perry and Green, 1984).

Although foams are metastable and will eventually collapse, foam breaking, achieved by chemical or mechanical means, is utilised to reduce the lifetime of the foam. Chemical defoaming methods involve the use of an antifoam agent, typically silica based, which work by reducing the stability of the thin liquid films (lamellae) within the foams structure (Kralchevsky *et al*, 2002). Hence chemical antifoams also function as foam inhibitors. Boiler feedwater is dosed with such antifoam agents to prevent foam formation within the boiler. Mechanical foam breakers, including turbine, vaned disk and paddle blades, destroy foam by inducing rapid pressure change and applying shear and compressive forces to the foam leading to bubble rupture. Ultrasound is essentially a mechanical foam breaking method, albeit one which is not widely used, with a varying pressure field acting upon the foam. The use of ultrasound in destroying foams is advantageous as the method is non-invasive and no chemical contaminants have to be added to the system.

Previous research, Sandor and Stein (1993), Morey *et al* (1999), Dedhia *et al* (2003) has demonstrated that ultrasound increases the rate at which foam collapses. However, conflicting conclusions as to why this increased collapse rate was observed have been drawn. Specifically, Dedhia *et al* (2003) contradict Sandor and Stein (1993) by refuting the increase in liquid drainage rate from foam subjected to ultrasonic vibrations. Sandor and Stein (1993) reason that this increase in liquid drainage rate is primarily responsible for the destruction of foam using ultrasound. The effect of ultrasound on liquid holdup (volume of liquid per volume of foam) is not discussed in the literature.

Electrical power supplied to the ultrasonic transducer in these papers was of the order of 25-110 Watts, compared to the 4 Watts used in the author's experiments. (Supply voltage was limited to 50v by health and safety constraints). All three studies positioned the ultrasonic transducer in air a distance of centimetres above the foam. The large impedance discontinuity between air and the lamellae of the foam means ~99% of the energy incident on the foam is reflected with this arrangement.

The aims of this project were to gain an appreciation of previous research concerning foam destruction using ultrasound in the literature and to determine, for the first time within Oxford University's Department of Engineering Science, whether ultrasound has a repeatable, observable effect on foam at useable power levels. An experimental set-up was developed through insight gained from preliminary work using an ultrasonic cleaning bath, in which foam was formed and observed. Consideration was also given to coupling between the ultrasound (27.72kHz and 40.00kHz) and foam. Height and liquid drainage were measured for static foam with two different initial liquid holdups, results being interpreted in terms of the two different rupture mechanisms identified by Monin, Espert and Colin (2000); Homogeneous rupture and so-called Front rupture.

Several previous fourth year projects have explored foam fractionation as a separation technique, the process being refined this year to incorporate reflux. One hindrance to this work is collapsing the foamate efficiently in order to obtain the enriched solution required to provide reflux for the foam column. At present mechanical, rotary, foam breakers are used which generate a significant quantity of unwanted stable secondary foam. An elegant ultrasound based method for collapsing foam would solve the problems associated with the current inability to completely destroy foam as it exits the fractionation column.

2.Foams:

2.1 Background:

Foams are an example of minimum surface structures. In fact thin, single soap films created between a wire frame are surfaces of zero mean curvature and hence of minimal surface (Weaire and Hutzler, 1999). Interestingly these soap film surfaces are useful in illustrating solutions to Plateau's problem, which is concerned with finding a surface of minimal area that spans a given contour in space.

This project is concerned with aqueous foams. A suitable definition of which is, a two-phase system in which a large volume fraction of gas is dispersed as bubbles throughout a continuous liquid matrix (Narsimhan and Wang, 2005 and Weaire and Hutzler, 1999). To elaborate, these gas bubbles are contained by thin liquid films stabilised by the presence of some form of surfactant (surface active molecules which preferentially accumulate at the liquid-gas interface). These films are interconnected at their meeting points via Plateau borders, forming a continuous liquid phase throughout the structure. Foam stability is governed by drainage properties and coarsening (also referred to as Ostwald ripening). In certain circumstances foam will undergo topological transformation to attain a state of lower surface energy, dissipating the excess energy as heat.

2. 2 Foam structure:

Figure 2.2.1 illustrates a typical foam structure.

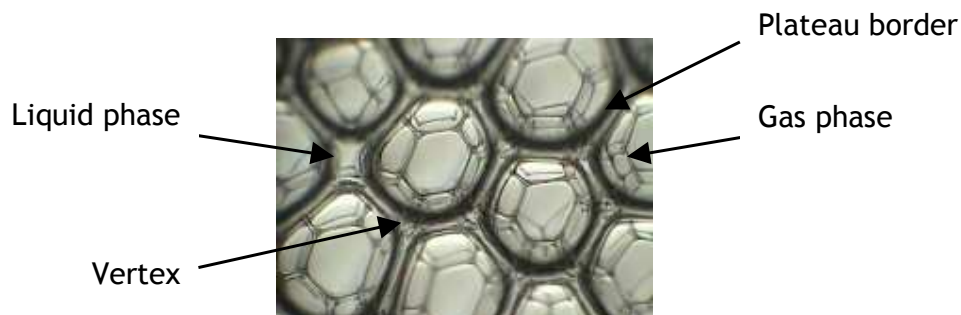
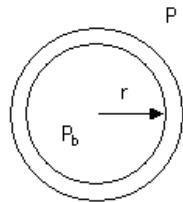


Fig 2.2.1- Foam Structure.

The structure of particular foam varies depending on the liquid fraction the foam contains. Wet foam consists of approximately spherical bubbles, separated by thick liquid films. In the limit of perfectly spherical, close packed (cubic or hexagonal) gas bubbles, the gas fraction in the foam is ≈ 0.74 . This results from the geometry of the foam and is mathematically stated by Keplers Conjecture, this problem being studied by mathematician Carl Gauss. In dry foam polyhedral gas cells are separated by thin liquid films named 'lamellae'. These lamellae intersect to form Plateau borders at angles of 120° . The 120° angle is a consequence of the required equilibrium of forces acting at the intersection due to surface tension of the lamellae. Connections between Plateau borders and adjacent liquid films are smooth.

2.3 Laplace equilibrium

The local equilibrium of a gas-liquid interface is governed by the Laplace equation. The Laplace equation relates the pressure difference across the interface to its surface tension. Equation 2.1 results from a force balance on the spherical bubble shown below figure 2.3.1:



$$P_b - P = \frac{4\gamma}{r} \quad (2.1)$$

P - Pressure outside gas bubble

P_b - Bubble pressure

r - Radius of curvature

Fig 2.3.1 Gas Bubble

This relationship shows us that at constant P (i.e. at atmospheric conditions) P_b increases as bubble radius decreases. Laplace's law can be used to explain the drainage of liquid from the lamellae into Plateau borders, from which the interstitial liquid flows down through the interconnected Plateau border network under the influence of gravity. Also the higher internal (Laplace) pressure of bubbles with small radii provides a driving force for the diffusion of gas through the lamellae into larger radii bubbles. This gas diffusion results in the average bubble radius of a particular foam sample increasing with time, an effect called Ostwald ripening or coarsening (Lim and Barigou, 2005). The gas diffusion process is slow compared to other foam collapse mechanisms, with bubble size actually increasing as time raised to the power half, $t^{1/2}$, (Monin *et al*, 2000). There is no change in the total quantity of gas entrained in the foam as coarsening occurs.

The Laplace equation does have limitations, for example problems can occur if viscous drag effects have to be accounted for, i.e. when subjecting foams to shear forces (Marze *et al*, 2005).

2.4 Surface active agents (Surfactants):

Surfactants are molecules that are amphiphilic, meaning they possess a hydrophilic 'head' and a hydrophobic 'tail' (Weaire and Hutzler, 1999). When present in foams surfactant molecules align themselves across the lamellae (see figure 2.4.1), satisfying both ends of the molecule, whilst improving the stability of the film by a variety of mechanisms, including lowering its surface tension (Barigou and Davidson, 1994).

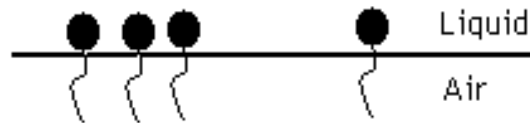


Fig 2.4.1 - Surfactant molecule accumulation at a liquid air interface.

Surfactants commonly utilised in foam generation include detergent, sodium dodecyl sulphate (SDS), whey protein, bovine serum albumin and triton-X-100 (Dedhia *et al*, 2004, McDaniel and Holt, 2000 and Barigou and Davidson 1994). Figure 2.4.2 shows the chemical formulae and molecular structures (Note the long hydrocarbon 'tails') of SDS and Triton-X-100.

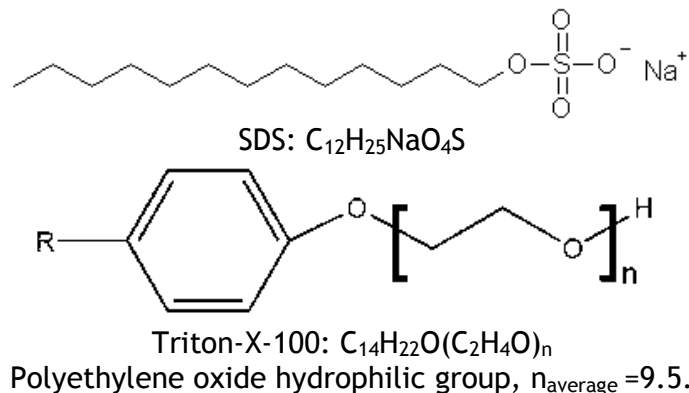


Fig 2.4.2 - Chemical composition and molecular structure of Surfactants.

There is a limit to the number of surfactant molecules that can be adsorbed to the liquid-gas interface before its surface becomes fully saturated. The concentration of surfactant at which this occurs is termed the Critical Micelle Concentration (CMC). Assuming the surfactant causes a reduction in film surface tension then the surface tension of the liquid film is at a minimum at this point. Figure 2.4.3 shows the general relationship between surfactant concentration and film surface tension, γ .

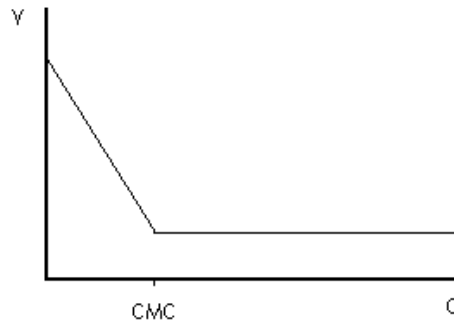


Fig.2.4.3 - Surface tension vs. surfactant concentration.

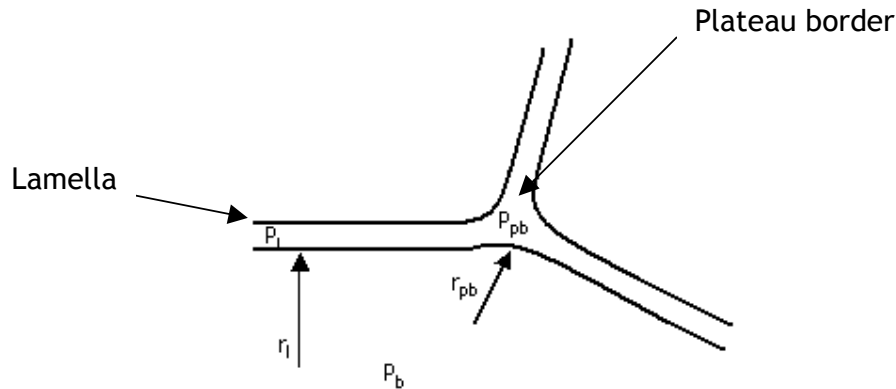
The mechanisms by which surfactants stabilise thin liquid films, such as those in existence in foams, are named the Marangoni effects. These effects are best understood by considering the relationship between surfactant concentration and surface tension of a single liquid film. Local thermal and mechanical perturbations cause local thinning of the liquid film, potentially leading to rupture. At this local thinning the liquid-gas interface is depleted of surfactant molecules, creating a surfactant concentration gradient and hence an opposing surface tension gradient. This surface tension gradient draws the film together, preventing rupture (Perry and Green, 1984). Marangoni effects also resist liquid drainage from lamellae, reducing instability. Long surfactant molecules, such as bovine proteins, provide extra stability as they can entangle and form a physical network across the liquid film, providing a physical resistance to liquid drainage and hence thinning.

2.5 Foam drainage and stability:

Foam is a thermodynamically unstable material, as foam generation actually results in an increase of the Gibbs free energy of the system (Narsimhan and Wang, 2005). Thus it is expected that foam of any composition will collapse given sufficient time.

Individual gas bubbles within a foam burst when their lamellae reach a critical thickness (Sandor and Stein, 1993), the actual rupture of the film often being caused by thermal perturbations. Lamellae reduce in thickness as liquid drains from them into the Plateau borders. Liquid flows through the interconnected Plateau border network under the influence of gravity so that the total liquid fraction present in the foam per unit volume (liquid holdup) reduces with time.

This drainage process from lamella to Plateau border can be understood by considering the Laplace equilibrium law, equation 2.1, at the lamella and at the Plateau border. This is shown in figure 2.5.1.



P_b - Bubble pressure

P_l - Pressure in lamella

P_{pb} - Pressure in Plateau border

r_l - Radius of curvature at lamella

r_{pb} - Radius of curvature at plateau border

$$P_b - P = \frac{4\gamma}{r} \Rightarrow r_l < r_{pb} \therefore P_l > P_{pb} \quad (2.1)$$

Fig 2.5.1 - Intersection of lamellae at a Plateau border.

Laplace's law shows that as radius of curvature reduces the pressure increases. As the radius of curvature of the lamella is much less than that of the Plateau border the pressure in the lamella is much greater than that in the Plateau border. The consequence of this pressure difference is a driving force, attempting to equalise the pressure difference, which acts on liquid in the lamella, causing it to drain into the Plateau border. This is known as Plateau border suction (Narsimhan and Wang, 2005).

The drainage equation, equation 2.2, (Weaire and Hutzler, 1999) provides a hydrodynamic model of liquid drainage and is used to describe the variation of liquid fraction of a foam as a function of position and time. The equation assumes Plateau borders are randomly orientated and that liquid holdup is comprised of some incompressible fluid (Monin *et al*, 2000). The second order term, which represents capillary effects, can be neglected until $a = 10^{-5}$.

$$\frac{\partial \alpha}{\partial \tau} + \frac{\partial}{\partial \xi} \left(\alpha^2 - \frac{\sqrt{\alpha}}{2} \frac{\partial \alpha}{\partial \xi} \right) = 0 \quad (2.2)$$

a - Dimensionless liquid fraction

ξ - Dimensionless vertical position

τ - Dimensionless time

3. Methods of Foam Breaking:

3.1 Background:

Many practical situations arise where the efficient destruction or inhibition of foam is necessary. These range from the destruction of foam to recover surface active species purified via foam fractionation, control of foam generated in aerated vessels such as fermenters to foam prevention in industrial steam boilers to prevent priming. Currently used defoaming techniques can be broadly separated into two categories; physical and chemical (Perry and Green, 1984). Common physical foam breaking methods involve mechanically transferring stress to the foam through some blade/paddle contacting process. Chemical defoaming methods involve the use of an antifoam agent, which can also function as a foam inhibitor, depending on where in a process it is introduced.

3.2 Physical foam breaking methods:

Different types of mechanical foam breakers, turbine, vaned disk and paddle blades, are shown in figure 3.2.1 (Takesono *et al*, 2002). These foam breakers destroy foam by inducing rapid pressure change and applying shear and compressive forces to the foam, leading to bubble rupture (Takesono *et al*, 2002). The use of mechanical foam breakers is more economical than chemical means as no expensive consumable antifoam agents are required. One significant draw back of traditional mechanical foam breakers is that their use results in the generation of stable secondary foam, a persistent, wet (high liquid holdup) foam consisting of gas bubbles that are significantly smaller than those of the primary foam (Gutwald and Mersmann, 1997).

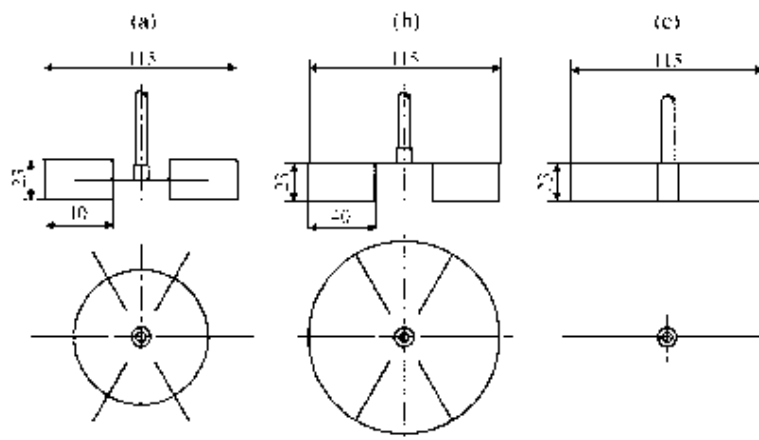


Fig 3.2.1- Mechanical foam breakers; a) six bladed turbine b) six bladed vaned disk c) two bladed paddle.

Ultrasound is essentially a mechanical foam breaking method, albeit one which is not used industrially, with a varying pressure field acting upon the foam. The use of ultrasound in destroying foams is advantageous as the method is non-invasive, doesn't result in chemical contamination and is potentially easy to integrate into existing processes.

3.3 Chemical defoaming methods:

Chemical antifoams typically consist of solid, hydrophobic filler particles dispersed in a silicone or hydrocarbon based oil that acts as a carrier (Kukarni *et al*, 1977). Although these oil and filler antifoam compounds are most efficient at destroying foams in certain circumstances either component can be used singularly. Hydrophobic Silica is commonly used as a filler at around 2-8 wt% (Kralchevsky *et al*, 2002). Discussion here is limited to the effect of antifoam compounds as in most cases these are most effective and provide a suitable benchmark to compare to mechanical foam breaking methods. Compound antifoams collapse foam by causing rupture of the lamellae (Kralchevsky *et al*, 2002). Lamellae rupture occurs as the hydrophobic filler particles effectively replace surface active molecules accumulated at the gas-liquid interface of the lamellae. This displacement of lamellae stabilising surface active molecules by the antifoam creates surface tension gradients disrupting the mechanical Laplace equilibrium, rupturing the foam bubble. Although both mechanical and chemical methods are invasive, chemical methods involve contamination with additional chemical species, meaning product purity and separation issues can be encountered.

4. Ultrasound:

4.1 Background:

The highest frequency that the human ear can detect is, on average (as there are slight variations from person to person and between age groups), 20kHz (Howard and Angus, 2006). Any sound generated above this upper limit is referred to as *ultrasound*. Ultrasound has a wide range of applications including medical imaging, sonar, non-destructive materials testing, foam generation and foam destruction (Ensminger and Dekler, 1973, Lim and Barigou, 2005 and Sandor and Stein 1993). Ultrasound is generated using a piezoelectric material that is typically incorporated into an ultrasonic transducer, driven by a signal generator.

4.2 Piezoelectric effect:

The piezoelectric effect occurs in crystalline solids with unit cells that do not have a centre of symmetry and was first demonstrated by the Curie brothers in 1880 (Blitz, 1956). Piezoelectric materials commonly used in ultrasonic transducers are Lead Zirconate Titanate and Barium Titanate; these are both ceramics (Channel Industries, 1999). When a piezoelectric material is subjected to a mechanical strain it will produce an electrical charge. Of more relevance to the generation of ultrasound is the reverse effect, the occurrence of mechanical strain when an electrical field is applied to the material (achieved by inducing equal and opposite charges on a pair of plane faces). Figure 4.2.1 shows the charge developed on opposing plane faces of a piezoelectric material when subjected to various stresses (Blitz, 1956).

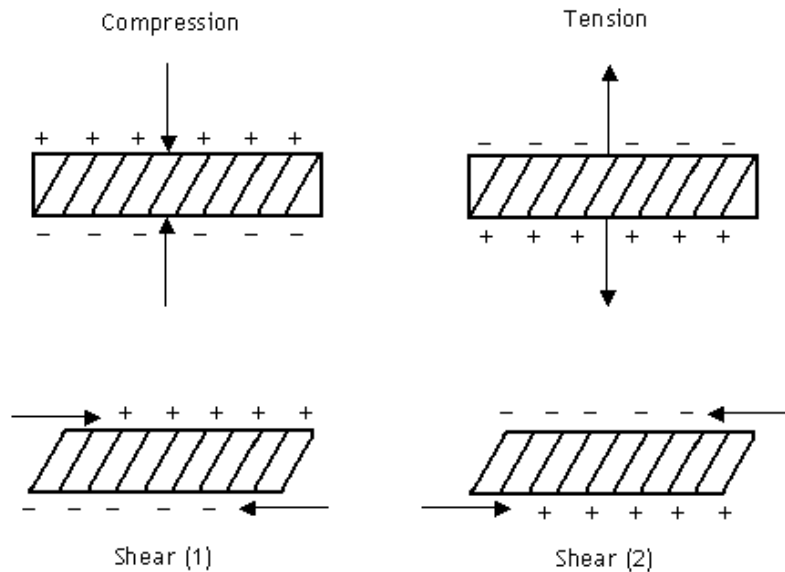


Fig 4.2.1 - Piezoelectric effect for different orientations of applied force.

The piezoelectric effect is quantified using the d coefficient (Blitz, 1956) measured in CN^{-1} or Vm^{-1} , equation 4.1:

$$d = \frac{q}{F} \quad d = \frac{V}{l} \quad (4.1)$$

- q - Value of total charge flowing
- F - Applied force producing stress
- V - Voltage applied across plane faces
- l - Displacement of crystal faces

The ceramic materials mentioned previously must be subjected to an operation referred to as 'poling' before they exhibit piezoelectric properties (www.channelindustries.com). This is due to the fact that in their natural state ceramic materials are isotropic and not polarised. The poling operation involves subjecting the material to a temporary static electric field that aligns the Weiss domains (locally aligned dipoles within the material) in the crystal structure. The result of this operation is that the material retains some polarisation and will now show piezoelectric properties.

4.3 Transducers:

A transducer is a device that converts one form of energy to another. In the case of ultrasonic transducers electrical energy is converted to mechanical energy. A common ultrasonic transducer design is the Langevin-sandwich, which consists of active piezoelectric elements sandwiched between two metal masses (Blitz, 1956 and Ensminger and Dekler, 1973). A common configuration is shown in figure 4.3.1.

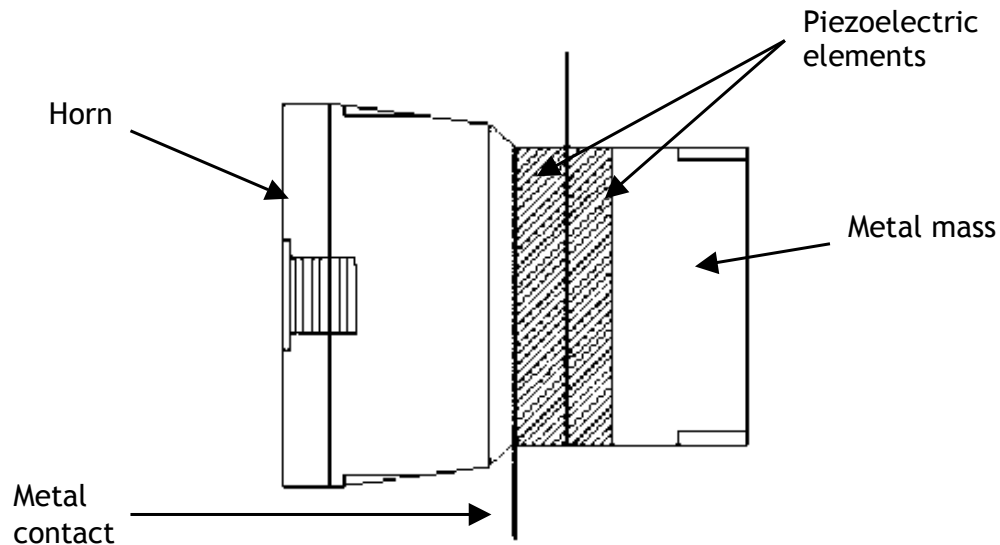
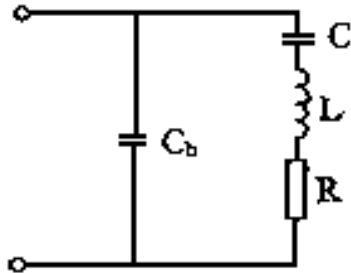


Fig 4.3.1 - Typical Transducer Design.

Several aspects of this transducer design make it advantageous. Firstly the metal masses lower the fundamental resonant frequency as well as acting as electrodes. This means transducers can be designed (i.e. masses chosen to enhance resonance, in terms of increasing the mechanical ' Q ' factor of the arrangement) to achieve resonance at a particular frequency of interest. Secondly the masses also act as a heat sink. This is vital as the piezoelectric elements cannot be allowed to reach the Curie temperature, the temperature at which the piezoelectric effect vanishes (Blitz, 1956).

The electromechanical properties of a transducer can be represented the equivalent circuit shown below in figure 4.3.2. The parallel capacitance can be chosen to increase the electrical 'Q' or change the resonant frequency at the expense of a high 'Q', the latter procedure being referred to as 'pulling' the resonant frequency of the piezoelectric crystal.



- C_a - Equivalent capacitance of mechanical circuit
- L - Equivalent inductance of mechanical circuit
- R - Represents mechanical losses and also acoustic power dissipated
- C_b - Electrical capacitance as described above

Fig 4.3.2 - Transducer equivalent electrical circuit (for frequencies around the first resonant peak) (Morgan Electroceramics).

The values of the components in the equivalent circuit can be determined by considering the resonant equivalent circuit and from a plot of impedance against frequency (determined experimentally by measuring the voltage drop across the transducer and current supplied, allowing impedance to be calculated, whilst sweeping the supply frequency). A typical characteristic plot is shown below in figure 4.3.3.

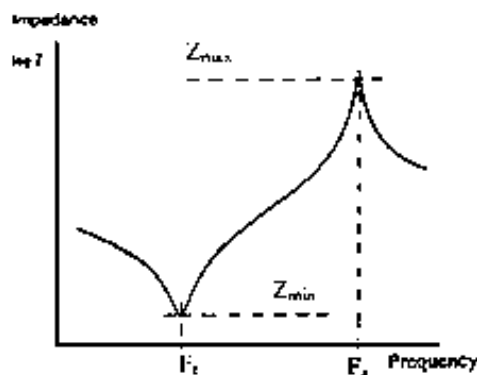


Fig 4.3.3 - Typical Impedance vs. Frequency plot for an ultrasonic transducer (Morgan Electroceramics).

The characteristic plot shows that at resonance (frequency F_r) the impedance of the system is at a minimum. Electrical resonance can be defined as a state when the energy stored by both capacitive and inductive elements is equal, hence allowing energy to 'shuttle' between these components (McKenzie Smith *et al*, 2002). For a parallel resonant circuit such as that shown in fig 4.3.2 the network resonates when V and I are in phase leading to equation 4.2:

$$F_r = \frac{1}{2\pi} \sqrt{\frac{1}{LC_a} - \frac{R^2}{L^2}} \quad (4.2)$$

However as impedance is at a minimum at F_r the following approximation can be made, yielding equation 4.3:

$$\frac{R^2}{L^2} \ll \frac{1}{LC_a} \Rightarrow F_r \approx \frac{1}{2\pi} \frac{1}{\sqrt{LC_a}} \quad (4.3)$$

As C_a is determined by the geometry and material properties of the piezoelectric element the above equation allows L to be calculated. The effect of the electrical capacitance, C_b , is to introduce a second resonant peak at frequency, F_a , that occurs at a maximum impedance. Equation 4.4 relates equivalent circuit parameters to frequency at this point:

$$F_a = \frac{1}{2\pi} \sqrt{\frac{C_a + C_b}{LC_a C_b}} \quad (4.4)$$

The signal chain for driving an ultrasonic transducer is illustrated in figure 4.3.4. A signal generator provides an oscillating signal which is amplified to the voltage required to drive the transducer. The drive circuit tunes the transducers resonance to improve the 'Q' factor and also contains a resistive element to ensure the output impedance of the drive circuit is matched to the transducers impedance at resonance, maximising power transfer.

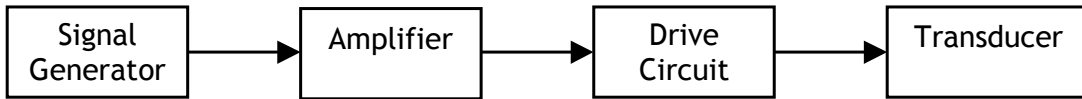


Fig 4.3.4 - Block diagram of ultrasonic transducer arrangement.

4.4 Impedance boundaries:

The effect of an ultrasonic transducer is to create pressure variations in the surrounding medium that vary with time, causing wave propagation. The wave equation, equation 4.5, (Howatson *et al*, 1991) is used to mathematically describe wave propagation (3-D):

$$\frac{\partial^2 u}{\partial t^2} = c^2 \nabla^2 u \quad (4.5)$$

The travelling wave solution to the wave equation in 1-D is given by equation 4.6:

$$y(x, t) = Ae^{j(\omega t - kx)} \quad (4.6)$$

As the ultrasound wave travels through a lossy medium it is attenuated due to viscous damping. If a travelling wave is incident on an impedance boundary a proportion of the wave's energy will be reflected from the discontinuity and the rest transmitted to the second medium. The impedance a material presents to the propagation of sound waves is named 'specific acoustical impedance', analogous to electrical impedance, and is defined as the ratio of acoustic pressure to velocity (of the sound wave), equation 4.7 (Blitz, 1956).

$$Z_a = \frac{P}{u} \quad (4.7)$$

The effect of an impedance boundary on a plane travelling wave (of the form described above) with normal incidence can be quantified by the coefficients of reflection and transmission. Figure 4.4.1 illustrates the arrangement of a plane wave incident upon an impedance boundary.

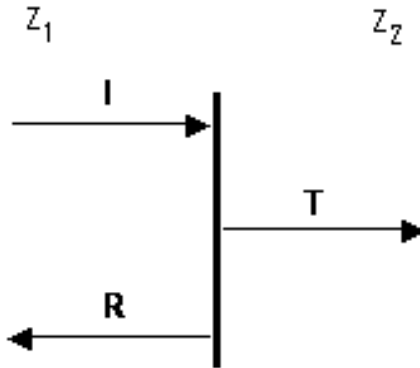


Fig.4.4.1-Impedance boundary and incident, reflected and transmitted waves.

The transmission, T , and reflection, R , coefficients are defined below, equations 4.8 and 4.9 respectively (Brady, 2004):

$$T = \left| \frac{T'}{I} \right| = \frac{4Z_1^2}{(Z_1 + Z_2)^2} \quad (4.8)$$

$$R = \left| \frac{R'}{I} \right| = \frac{(Z_1 - Z_2)^2}{(Z_1 + Z_2)^2} \quad (4.9)$$

Obviously the wave is continuous across the boundary; the incident and transmitted waves are always in phase whereas a phase change can occur between the incident and reflected waves.

5. Foam-ultrasound interaction:

5.1 Coupling between foam and ultrasound:

Coupling from the medium that ultrasound is travelling to another is most efficient when there is no discontinuity in acoustical impedance (see equation 4.7) (Blitz, 1956). This is a distinct problem when foam is considered, as, in a simplistic sense, foam is a series of air/water boundaries. Taking typical values for the specific acoustical impedance of air ($430 \text{ kgm}^{-2}\text{s}^{-1}$) and water ($1.5 \times 10^6 \text{ kgm}^{-2}\text{s}^{-1}$) (Blitz, 1956) and considering a plane wave at normal incidence to the air/water boundary the reflection coefficient is found from equation 4.9:

$$R = \left| \frac{R^i}{I} \right| = \frac{(Z_1 - Z_2)^2}{(Z_1 + Z_2)^2} = \frac{(1.5 \times 10^6 - 430)^2}{(1.5 \times 10^6 + 430)^2} \approx 0.9989 \quad (4.9)$$

This extremely large reflection coefficient means that $\approx 99\%$ of ultrasound incident on a foam will simply reflect from the foam surface and not interact with the foam in any significant manner. This leads to the expectation that ultrasound will not propagate very far into the bulk of a foam due to reflection from impedance boundaries. Attenuation of the travelling wave will further limit the depth of propagation.

Experiments conducted by Sandor and Stein (1993) and Morey *et al* (1999) both utilise similar apparatus; an ultrasonic transducer (20kHz) positioned axially, above a column containing foam which is generated in situ. A distance of the order of centimetres is kept between the vibrating surface of the transducer and the top surface of the foam. The apparatus used by Morey *et al* (1999) is shown in figure 5.1.1 (no diagram was provided by Sandor and Stein (1993)). With this setup the high reflection coefficient due to the impedance discontinuity makes it difficult to determine the energy transferred to the foam by the ultrasound. Only qualitative conclusions such as those made by Sandor and Stein about the dependence of foam stability on electrical power delivered to the transducer can be drawn. Nothing can be said about the energy required to actually collapse the foam itself. This is an experimental problem that requires rectification to allow further insight into foam collapse stimulated by ultrasound to be gained.

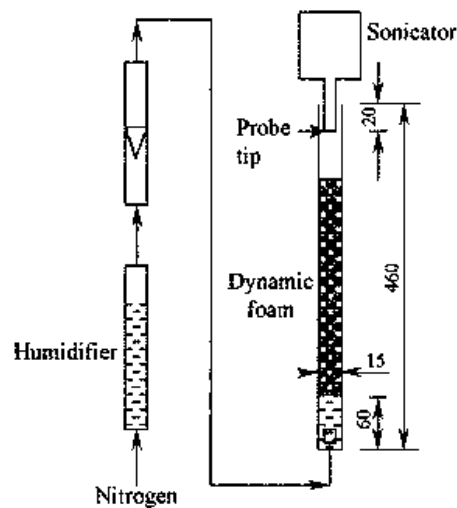


Fig 5.1.1-Experimental Apparatus used by Morey *et al.*

Unfortunately it is not clear from previous research how ultrasound interacts with the continuous liquid phase in the foam. Only Dedhia *et al* (2003) draw attention to the issue of the large reflection coefficient at the air/foam boundary. Again Dedhia *et al* (2003) use 20kHz ultrasound, lower than either of the two frequencies used here, and two transducer arrangements, one in intimate contact with the foam, the other at a distance of 0.5 cm above the foam. Dedhia *et al* (2003) note that the collapse rate decreases as distance from the foam surface is increased. This observation is consistent with the understanding that attenuation occurs as the ultrasound waves propagate in a lossy medium (Brady, 2004). Bearing previous work in mind it seems prudent to design apparatus with the ultrasonic transducer axially aligned with a foam column of comparable diameter to the diameter of the transducer face, but underneath the foam in a similar arrangement to that of an ultrasonic bath. It is intended that this setup will maximise the fraction of total foam volume that is influenced by the ultrasound and minimise the amount of reflection occurring.

5.2 Mechanisms of film rupture and the influence of ultrasound:

Once the issue of coupling between foam and ultrasound is negotiated, the actual mechanisms by which ultrasound destroys foam require consideration. Various ultrasound enhanced rupture mechanisms are suggested in the literature, although it is not apparent which mechanism best describes the actual collapse process. It is desirable to obtain experimental results that allow for differentiation between these possible rupture mechanisms.

Sandor and Stein (1993) propose that ultrasonic vibrations cause surface waves to develop in the lamellae within the foam structure, postulating that these waves will be of “squeezing” mode type, causing accelerated film drainage and leading to the liquid films reaching their critical thickness in a shorter time period, hence increasing the foam collapse rate. This postulate is referenced in the works of Morey *et al* (1999) and Dedhia *et al* (2003). It is important to distinguish between local drainage, which ultrasound has a direct influence on, and global drainage, the drainage of interstitial liquid from the bulk of the foam (observable as the reduction in average liquid holdup with respect to time). It is expected that liquid released by the rupture of lamellae will first be taken up by the surrounding Plateau borders rather than directly draining into the bulk of the surfactant solution. This accounts for the questions raised concerning the validity of Sandor and Stein’s model raised by Dedhia *et al* (2003) who recorded global liquid drainage via a manometer, measuring changes in static head with respect to time. Little change in global drainage was noted by Dedhia *et al* (2003) when the foam was subjected to ultrasound. Care must be taken when trying to measure foam drainage via pressure readings as the practicality and accuracy of manometer use in an environment with pressure gradients, due to the presence of ultrasound, is limited.

The work of Monin *et al* (2000) pertains directly to foam collapse (without the influence of ultrasound). Two distinct rupture mechanisms are identified; Homogeneous Rupture and Front Rupture. Homogeneous rupture refers to breaking of lamellae independent of position within the foam and hydrodynamic conditions. This process can be thought of as probabilistic and quantified in terms of a probability of lamellae rupture per unit time and unit surface, equation 5.1.

$$dN = \frac{1}{2} \pi D^2 N \omega dt \quad (5.1)$$

dN - Rupture events in time interval dt

N - Total number of bubbles

D - Average bubble diameter

ω - Probability of rupture per unit time and unit surface

As this process is independent of hydrodynamic conditions it is expected that ultrasound will not influence the homogeneous rupture of foam.

Front Rupture describes bubble collapse that occurs when lamellae reach a critical thickness. Films reach critical thickness after a certain amount of drainage has taken place (dependent on bubble diameter, the presence of surfactant(s) and lamellae viscosity). As global drainage progresses liquid holdup will reduce at the top or front of a foam first; hence a rupture front exists and, in the case of a vertical column of foam, will travel downwards as time progresses and bubbles rupture. As Front Rupture is stimulated by liquid drainage it is likely that ultrasound will alter this mode of foam collapse. More specifically, subjecting foam to ultrasound should cause critical thickness to be reached in a shorter time period, making Front Rupture the dominant mechanism of foam destruction.

Both the Homogeneous and Front Rupture mechanisms are explained by considering a single film drainage model known as the Derjaguin-Landau-Verwey-Overbeek (DLVO) theory (Monin *et al*, 2000). Essentially this theory describes the equilibrium of rigid film interfaces in terms of molecular interactions.

Barigou and Davidson (1993) present and compare a further two theories of single film drainage; Reynolds model of hydrodynamic lubrication and the Swept film surface model. It is found that the Reynolds model underestimates film drainage rates by several orders of magnitude and results in a description of the film pressure distribution that is parabolic with respect to radius. The inaccuracy is due to the assumption that the film is bounded by inextensible interfaces, which is not the case when fluid interfaces are to be considered i.e. liquid films within foams. The swept film surface model allows for fluid interfaces and splits the film into three sections, the static plateau border region, the transition region and the lamella region. All significant flow and viscous dissipation occurs in the transition region, where surfactant concentration varies from a minimum to a maximum at the exit of the region, with corresponding changes in the surface tension of the film.

6. Experimental Technique:

6.1 Ultrasound generation:

In order to investigate the frequency dependence of ultrasound induced foam collapse two different frequencies of ultrasound, 27.72kHz and 40.00kHz, were used. Ultrasound was generated using two similar Langevin-sandwich type transducers each with a different resonant frequency. See Appendix C for transducer pressure calibrations. Each transducer was driven by a sinusoidal voltage, 50 V_{p-p} (17.7 V_{rms}) the maximum that could be used due to health and safety constraints, via a Wavetek model 25 signal generator and a FLC electronics P200 linear amplifier with a voltage gain of 10, see figure 6.1.1. The average electrical power supplied to both transducers at resonance was approximately 4 W.

Each transducer (27.72kHz and 40.00kHz) was attached to a plastic 'cup' (see Appendix B for cup design) via a screw thread. The contact surfaces of the transducer and cup were bonded with epoxy resin to minimise any impedance boundaries due to air pockets, figure 6.1.2 shows this arrangement. The plastic cup provides a reservoir of surfactant solution from which foam is generated, meaning the ultrasound is transmitted to the continuous liquid phase of the foam without encountering any large air/water impedance boundaries until the air bubbles within the foam are met.

6.2 Surfactant solution makeup:

For all experiments a surfactant solution composed of 5 Vol. % Teepol detergent and 95 Vol. % deionised water was used. This solution was chosen as it is benign and was also used by Barigou and Davidson (1993) in their work concerning soap film drainage (see section 5.2). The single film surface tension of the surfactant solution was measured using a Krüss Tensiometer and found to be; $\sigma = 35.14$ mN/m, comparable to Barigou and Davidson's (1993) value; $\sigma = 35.00$ mN/m. The density of the solution was measured as $\rho = 1005$ kg/m³, whilst the value quoted by Barigou and Davidson (1993) was $\rho = 1006$ kg/m³.

6.3 Method of foam formation and liquid drainage/foam height measurements:

A photograph of the apparatus used in the author's experiments is shown in figure 6.3.1. This experimental set-up consisted of a glass column of height 420mm, internal diameter 75mm that was positioned vertically above the plastic cup surfactant reservoir and transducer assembly. Foam was generated using a metal air sparger, air being supplied by a Charles Austen Dymax 14 pump. Airflow rates were measured via a rotameter. The cylindrical metal air sparger comprised of 6 horizontally aligned 2mm diameter holes. A seal was formed between the air sparger and plastic cup using a rubber O-ring arrangement.

Experimental runs were conducted using no ultrasound, 27.72 kHz and 40.00kHz ultrasound for two different values of initial liquid holdup (experimentally it is extremely difficult to tightly control this variable). Initial liquid holdup was altered by generating foam using two different air flow rates; 1 L/min and 0.5 L/min respectively, the higher airflow rate giving a larger initial liquid holdup. These values of airflow rate were chosen as they represent the maximum possible airflow rate obtainable from the pump used and also the minimum airflow rate at which the foam column could be filled, hence giving the largest variation in initial liquid holdup achievable with this apparatus. Foam was generated to an initial height of 300mm (volume of $1.325 \times 10^6 \text{mm}^3$), at which point the air supply was terminated and ultrasound turned on (if required). Measurements of foam height and liquid drainage were taken manually at 30-second intervals. Foam height was measured using a ruler clamped vertically, adjacent to the foam column, and foam drainage was recorded by measuring the mass of liquid collected in a beaker, positioned on a top pan balance. Liquid was transferred to the beaker via the drainage line. Three repeats of each experiment were conducted to allow for trends to be established and any outliers to be identified.

Experiments were conducted in a random order to avoid introducing any systematic error, which could be caused by depletion of surfactant in solution between runs due to adsorption to the surfaces of the plastic cup.

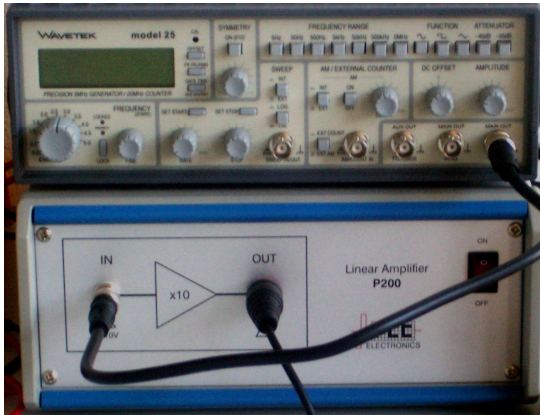


Fig 6.1.1- Wavetek signal generator and FLC electronics linear amplifier used to drive ultrasonic transducers.

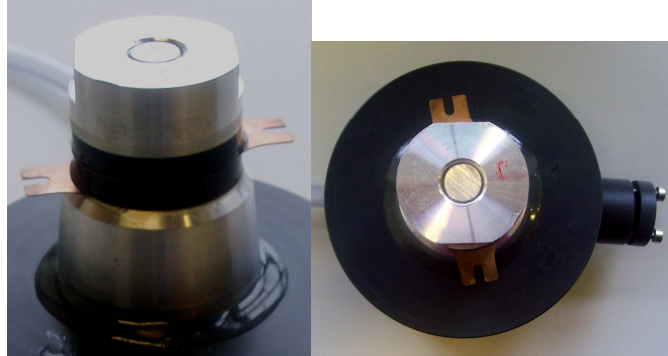


Fig 6.1.2- Side and plan views of underside of plastic cup arrangement showing 40.00kHz transducer and epoxy bonding.

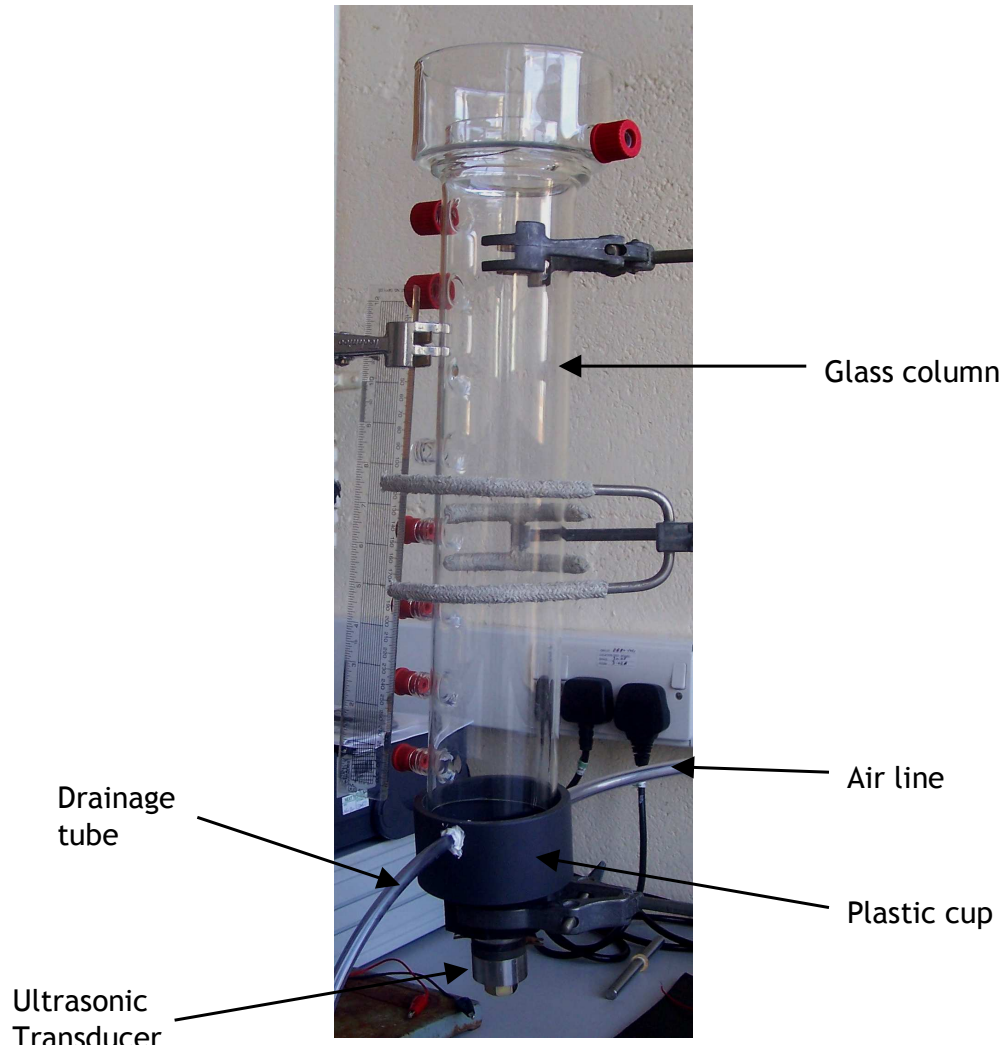


Fig 6.3.1-Complete Apparatus (no foam).

7. Results:

For all experiments an initial foam height of 300mm was generated by bubbling air through a surfactant solution composed of 5 Vol. % Teepol detergent and 95 Vol. % deionised water. Foam height and cumulative liquid drainage were directly measured during experiments.

Two complete sets of experiments were conducted. The first group of experimental runs measured foam height and cumulative liquid volume drained for foam generated using an airflow rate of 1 L/min, to achieve a high initial liquid holdup, and subjected to no ultrasound, 27.72kHz and finally 40.00kHz ultrasound. The second group of experiments followed the same procedure only using a lower airflow rate of 0.5 L/min, to generate foam with a lower initial liquid holdup. Bubble diameters were approximately constant between experiments at a particular airflow, however the dependence of bubble diameter on airflow rate gave rise to an undesirable change in bubble diameter between foams generated at the two different airflows. An airflow rate of 1 L/min produced foam with an approximate average bubble diameter in the range 7-8mm whilst the lower airflow rate of 0.5 L/min resulted in a range of bubble diameters 4-5mm.

7.1 Ultrasonic transducer calibrations:

The resonant frequency of each ultrasonic transducer was identified by measuring the voltages dropped across the transducer and an 18Ω series resistance. At resonance the transducer impedance is purely resistive and at a minimum, corresponding to a maximum in the voltage dropped across the series resistor. The values of resonant frequency measured were confirmed by observing the phase relationship between the transducer and resistor voltages on an oscilloscope (these voltages are in phase at resonance). For all measurements the transducer-resistor series circuit was supplied with a sinusoidal voltage of $50 V_{p-p}$ ($17.7 V_{rms}$) i.e. the voltage used in experiments. Figures 7.1.1 and 7.1.3 show the variation in the voltage dropped across the series 18Ω resistor with electrical supply frequency. Sharp maxima at 40.00kHz and 27.72kHz respectively are observed. Correspondingly figures 7.1.2 and 7.1.4 show the anticipated minimum in transducer impedance at resonance, in both cases a sharp increase in impedance is noted for frequencies just above resonance.

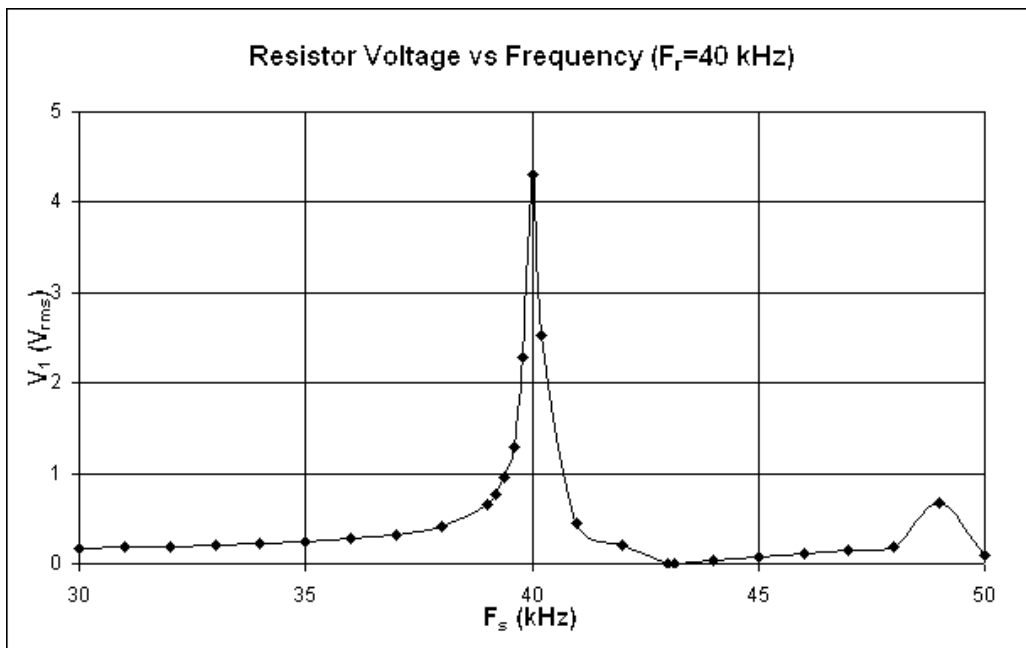


Fig 7.1.1 - Voltage dropped across series resistance vs. Supply frequency for 40.00kHz ultrasonic transducer.

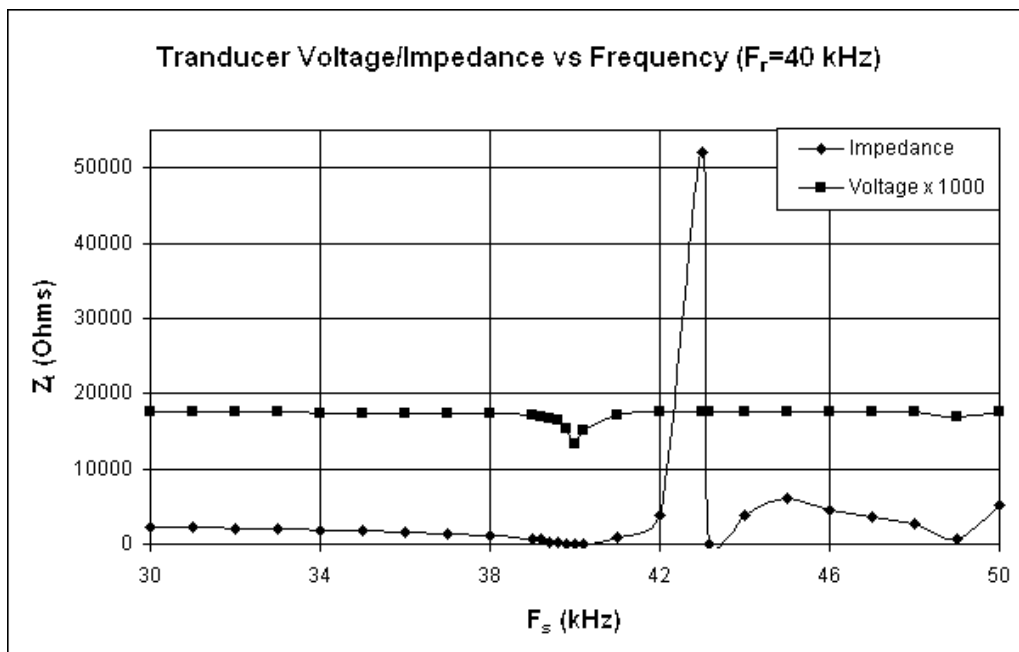


Fig 7.1.2 - Ultrasonic transducer impedance vs. Supply frequency for 40.00kHz ultrasonic transducer.

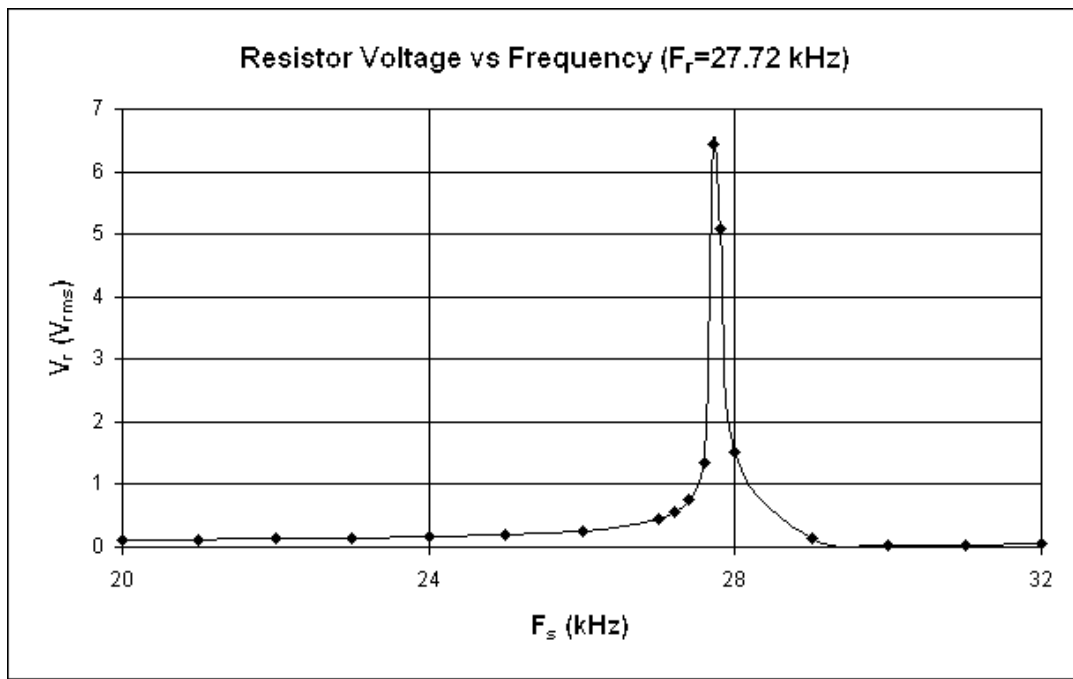


Fig 7.1.3 - Voltage dropped across series resistance vs. Supply frequency for 27.72kHz ultrasonic transducer.

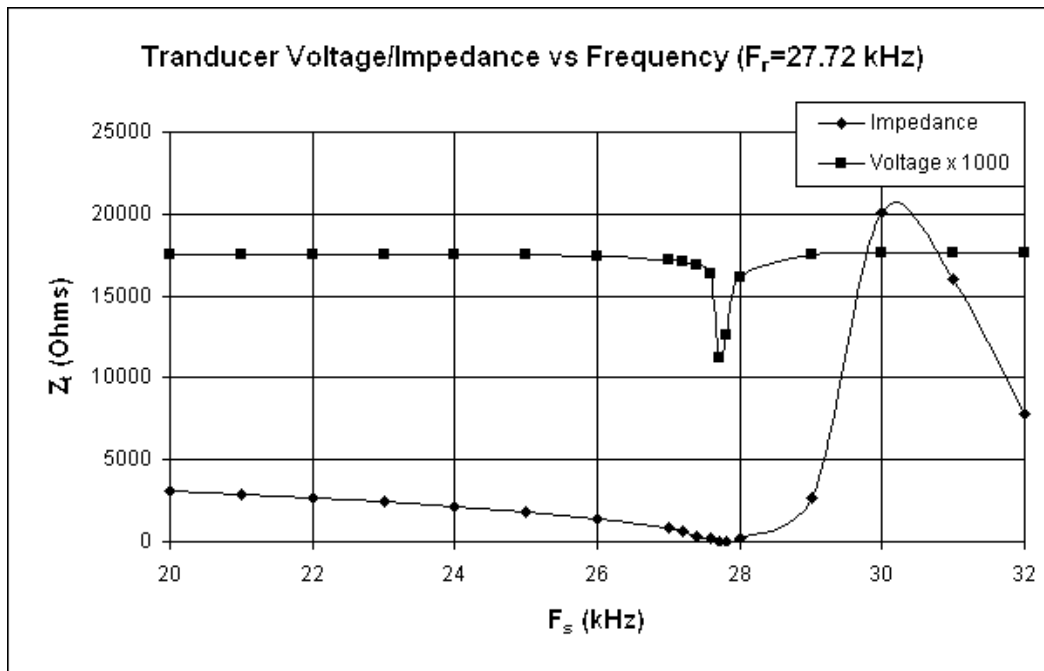


Fig 7.1.4 - Ultrasonic transducer impedance vs. Supply frequency for 27.72kHz ultrasonic transducer.

7.2 Cumulative liquid drainage:

Raw cumulative mass (g) of liquid drained data from all eighteen experiments undertaken is shown in figures 7.2.1 and 7.2.3. All of the curves obtained for no ultrasound, 27.72kHz and 40.00kHz ultrasound show similar general trends; an increase and gradual levelling of volume of liquid drained with time. Significant offsets exist between repeats due to limitations of the experimental method used. These limitations are discussed in section 7.8.

Plots of mean cumulative volume (ml) of liquid drained for two different initial liquid holdups are shown in figures in figures 7.2.2 and 7.2.4. These graphs are obtained from averaging the raw data for the three repeats of each no ultrasound, 27.72kHz and 40.00kHz ultrasound experimental run, shown in figures 7.2.1 and 7.2.3, and converting the measurements of liquid mass to volume by dividing by the surfactant solution density, 1005 kg/m^3 . The total volume of liquid drained was standardised by taking the mean across of the three experiments (no, 27.72kHz and 40.00kHz ultrasound) conducted at each initial liquid holdup. The total volume of liquid drained from the high initial liquid holdup foam was found to be 8.96ml, greater than that drained from the lower liquid holdup foam, 8.49ml, as expected. The reduction in initial global drainage for the 40.00kHz ultrasound case is surprising, given that drainage rates are simultaneously increased.

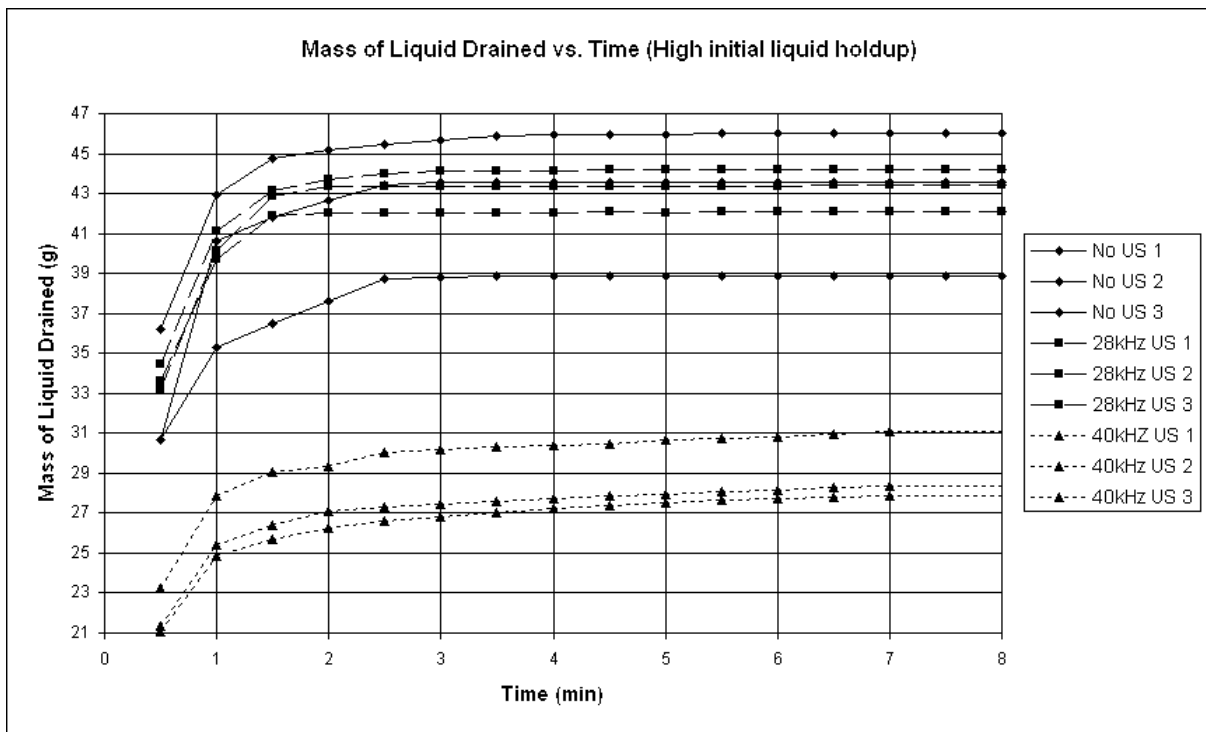


Fig 7.2.1-Raw liquid drainage data for high initial liquid holdup.

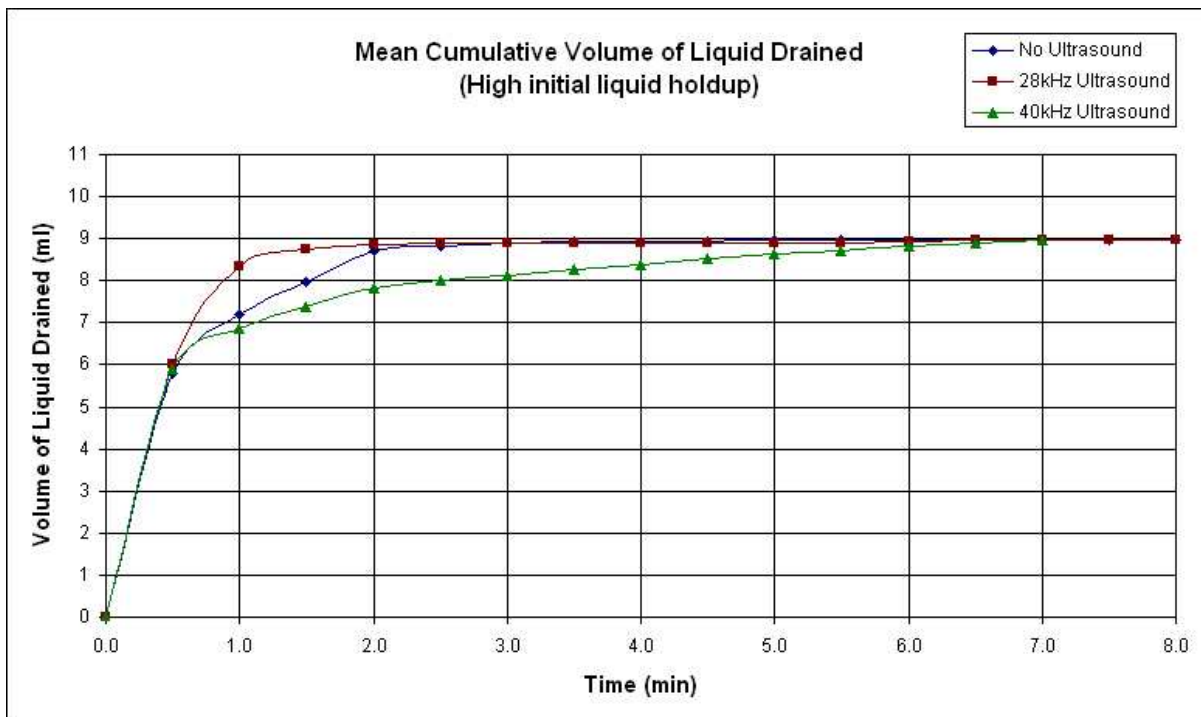


Fig 7.2.2-Plot of averaged experimental data showing variation of liquid drained from the foam with time for high initial liquid holdup.

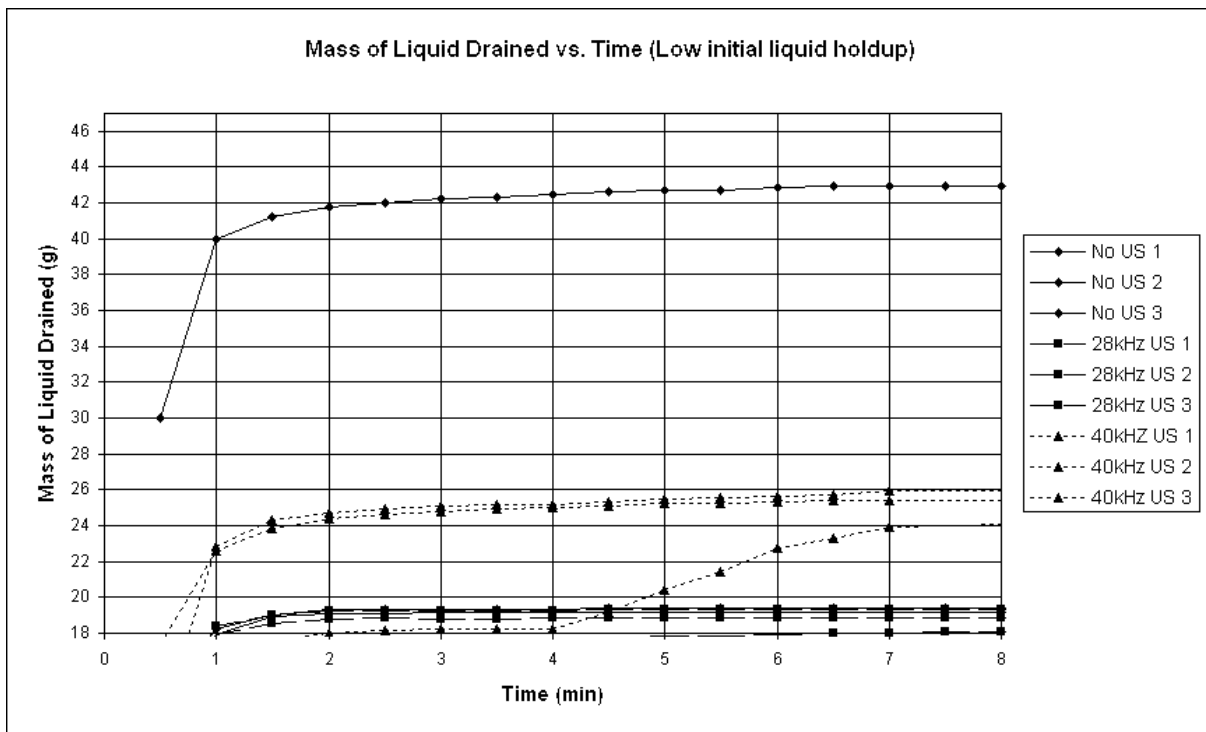


Fig 7.2.3-Raw liquid drainage data for low initial liquid holdup.

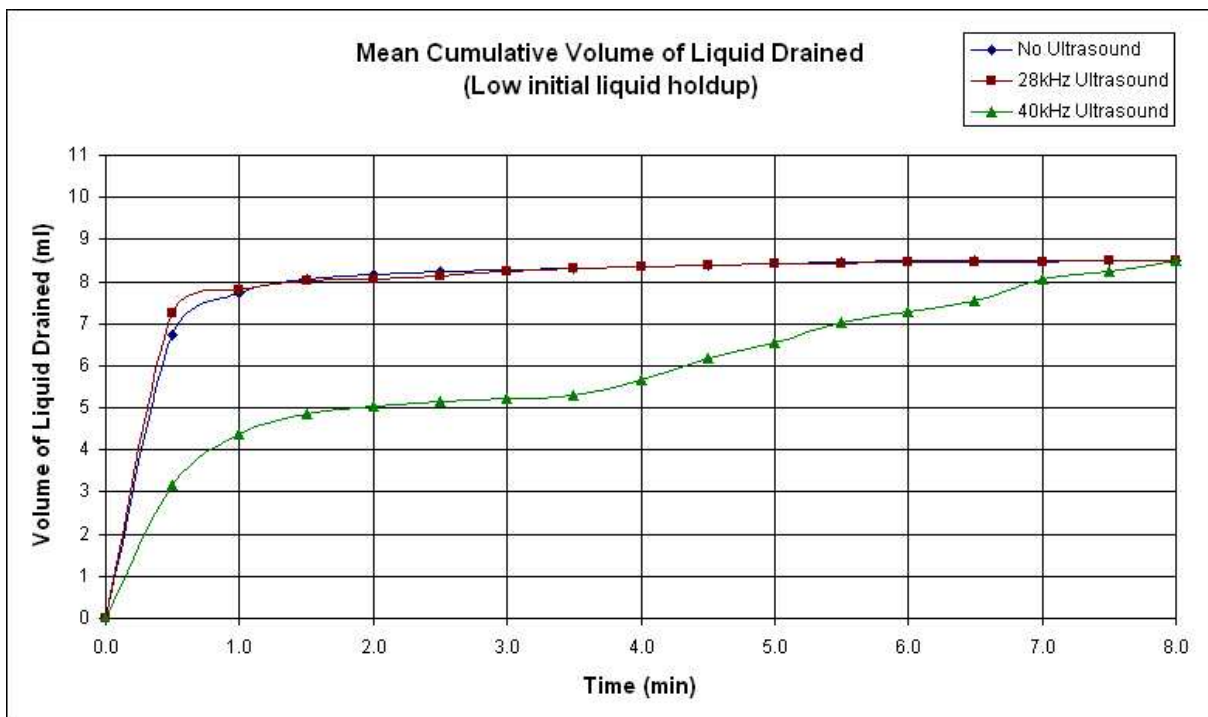


Fig 7.2.4-Plot of averaged experimental data showing variation of liquid drained from the foam with time for low initial liquid holdup.

7.3 Liquid drainage rate:

Drainage rate data for each experiment was obtained by numerically differentiating raw experimental measurements of volume of liquid drained with respect to time, shown in figures 7.3.1 and 7.3.4. Differentiating the liquid drainage data removes the experimental offset errors that were present in the raw data.

Figures 7.3.2 and 7.3.5 show the variation of average liquid drainage rate with time for two different initial liquid holdups. After initial transient behaviour (approximately the first 2 minutes), which exists due to initial experimental offset errors, a significant increase in liquid drainage rate is observed for the 40.00kHz ultrasound experiments. There is not sufficient evidence to confirm this observation for 27.72kHz ultrasound. The increase in liquid drainage rate caused by 40.00kHz ultrasound is clearer in figures 7.3.3 and 7.3.6, which show a magnified view of figures 7.3.2 and 7.3.5 after initial transient behaviour.

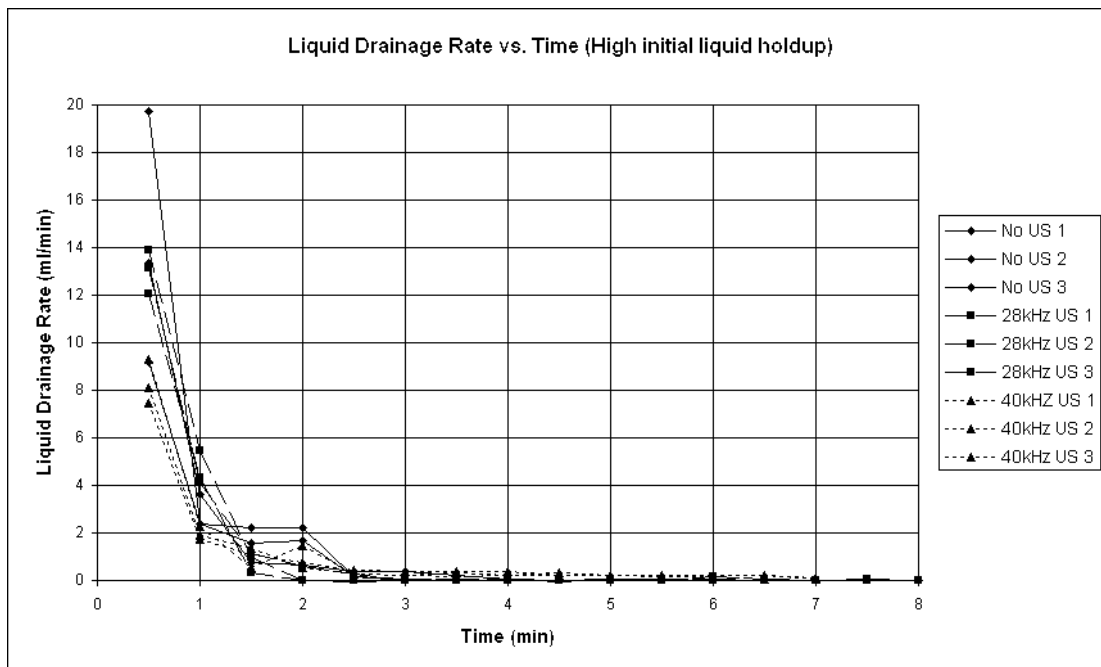


Fig 7.3.1-Liquid drainage rate data for high initial liquid holdup.

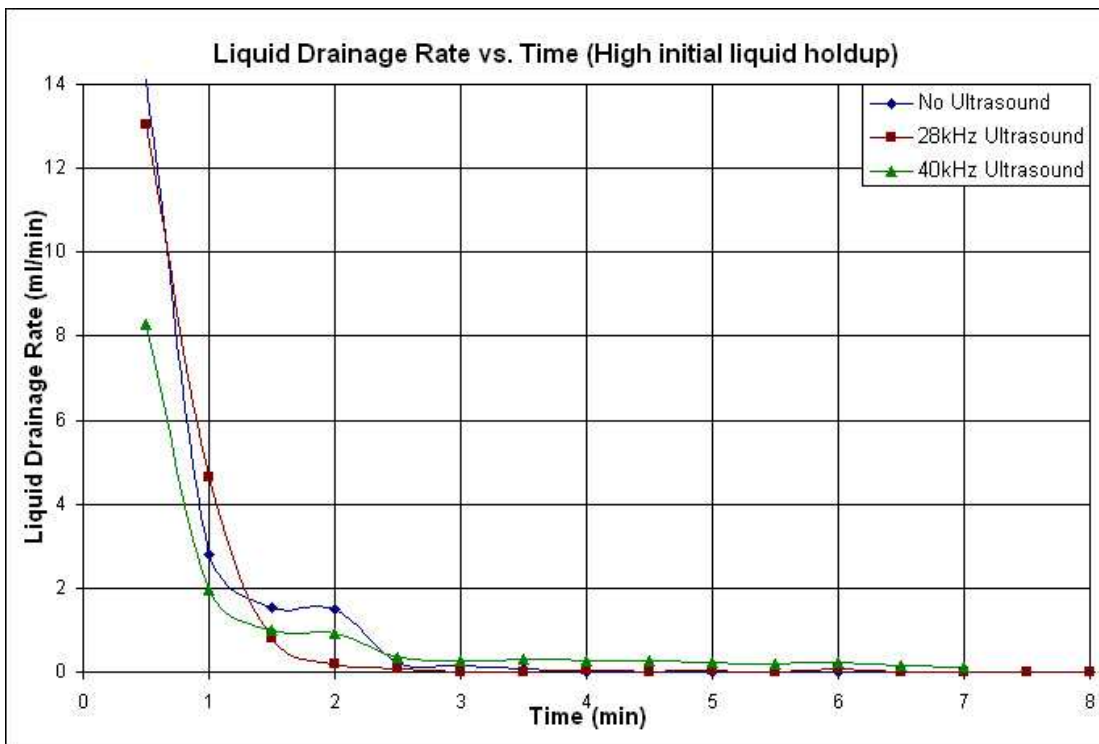


Fig 7.3.2-Drainage transients for foam with high initial liquid holdup.

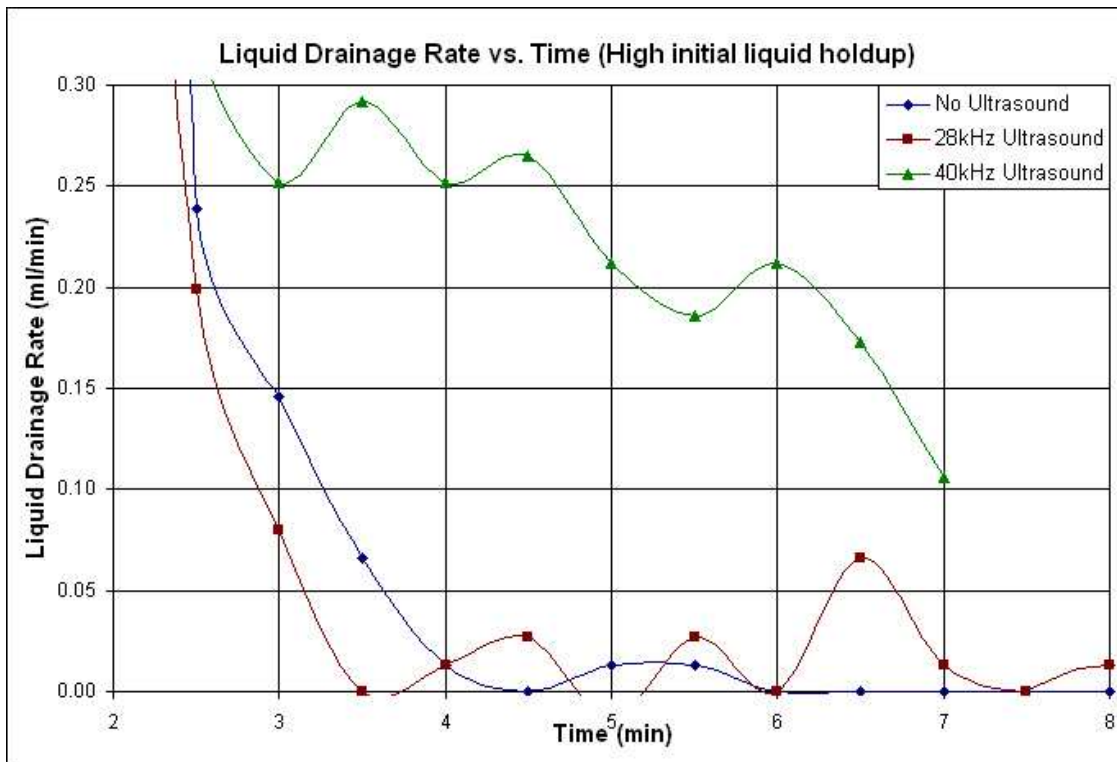


Fig 7.3.3-Magnified view of drainage transients for foam with high initial liquid holdup.

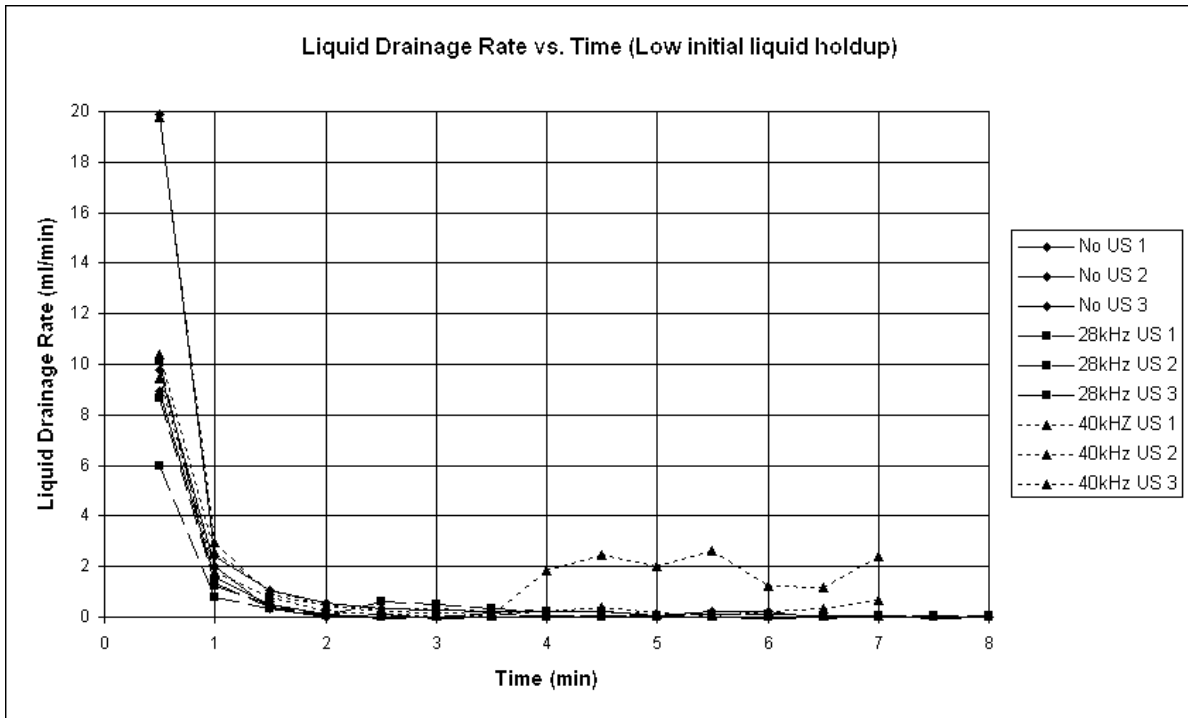


Fig 7.3.4-Liquid drainage rate data for low initial liquid holdup.

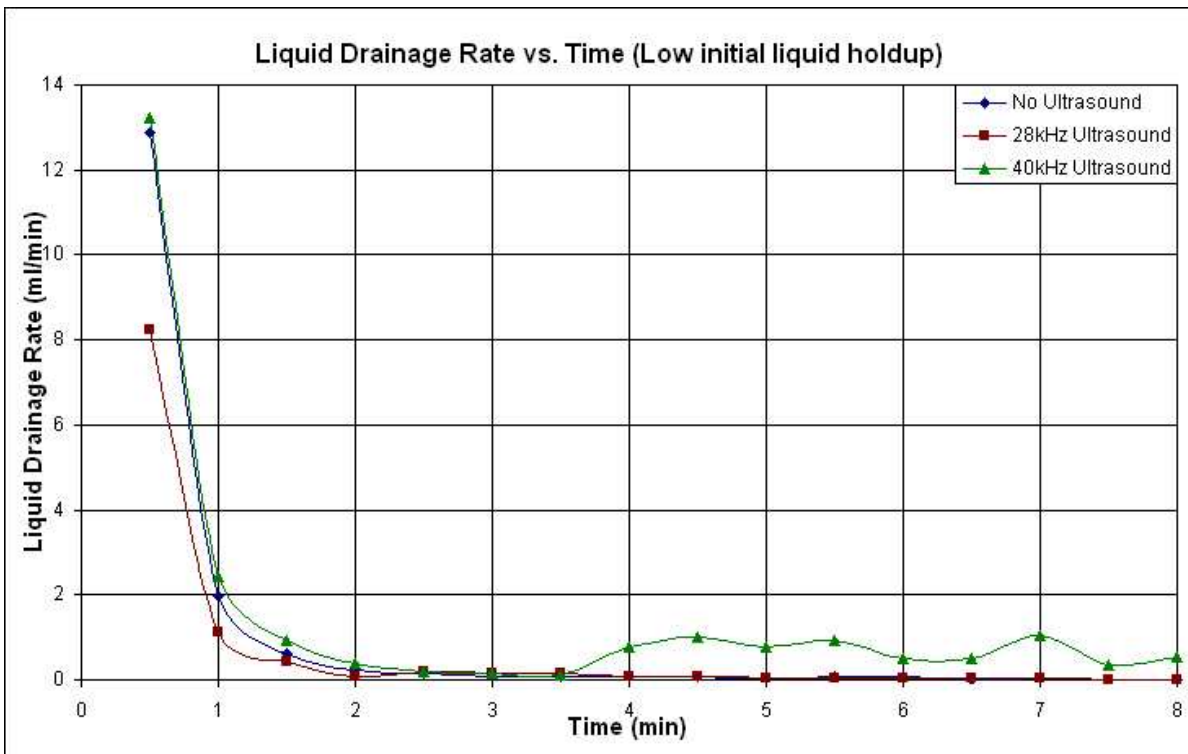


Fig 7.3.5-Drainage transients for foam with low initial liquid holdup.

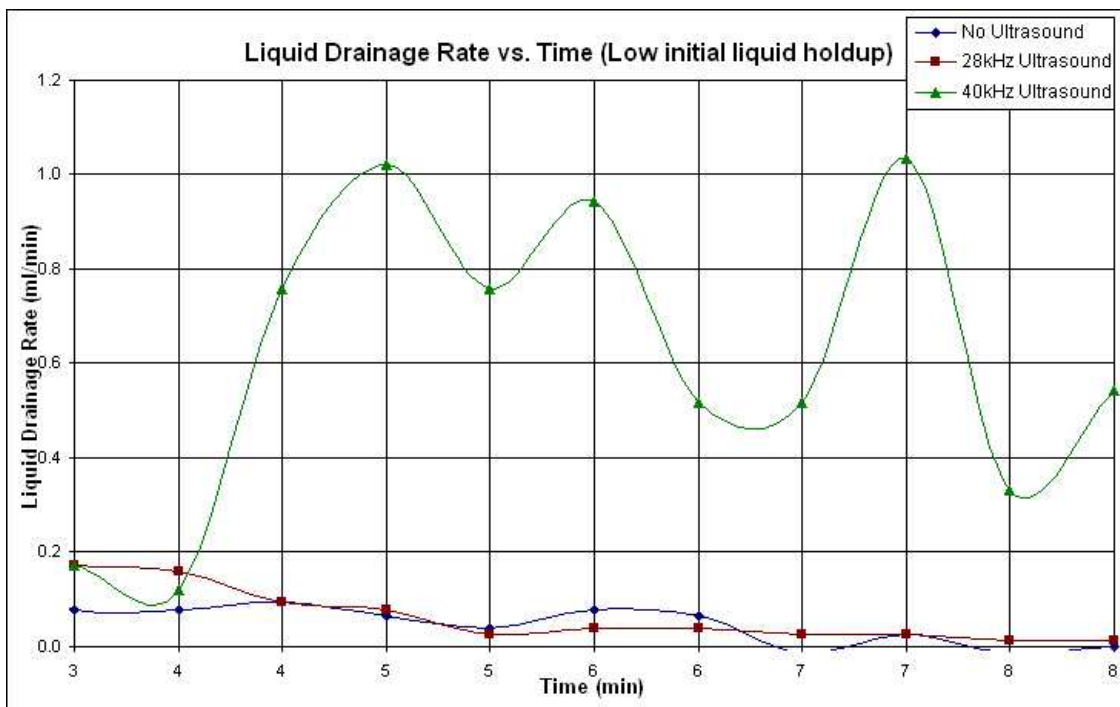


Fig 7.3.6-Magnified view of drainage transients for foam with high initial liquid holdup.

7.4 Foam height:

The raw data showing the variation of foam height (cm) with time for all experiments undertaken at each liquid holdup is shown in figures 7.4.1 and 7.4.2. Averages are taken over each data set of three repeats to obtain the mean foam height data.

The variation of mean foam height with time is shown in figures 7.4.2 and 7.4.4. Error bars indicate the standard error at each point. It was observed experimentally that for a high initial liquid holdup 40.00kHz ultrasound collapses foam in 7 minutes, a shorter period of time than the 8 minutes required for complete collapse in the case of 27.72kHz ultrasound or in the absence of ultrasound, see figure 7.4.1. The general trend of figure 7.4.2 shows that the foam head is smaller for foam subjected to 40.00kHz ultrasound. The same cannot be said for 27.72kHz ultrasound.

Figure 7.4.4 illustrates an observation made during experiments, foam of a lower initial liquid holdup is more persistent, complete collapse not occurring within 8 minutes, even in the case of 40.00kHz ultrasound. However this can be explained by the fact that generating foam of a lower initial liquid holdup is achieved by using a lower airflow rate (0.5L/min as opposed to 1 L/min). The result of the lower airflow rate being foam generation takes significantly longer, during which time drainage, bubble rupture and coarsening of the foam occur, leading to surfactant enrichment and hence a more stable foam.

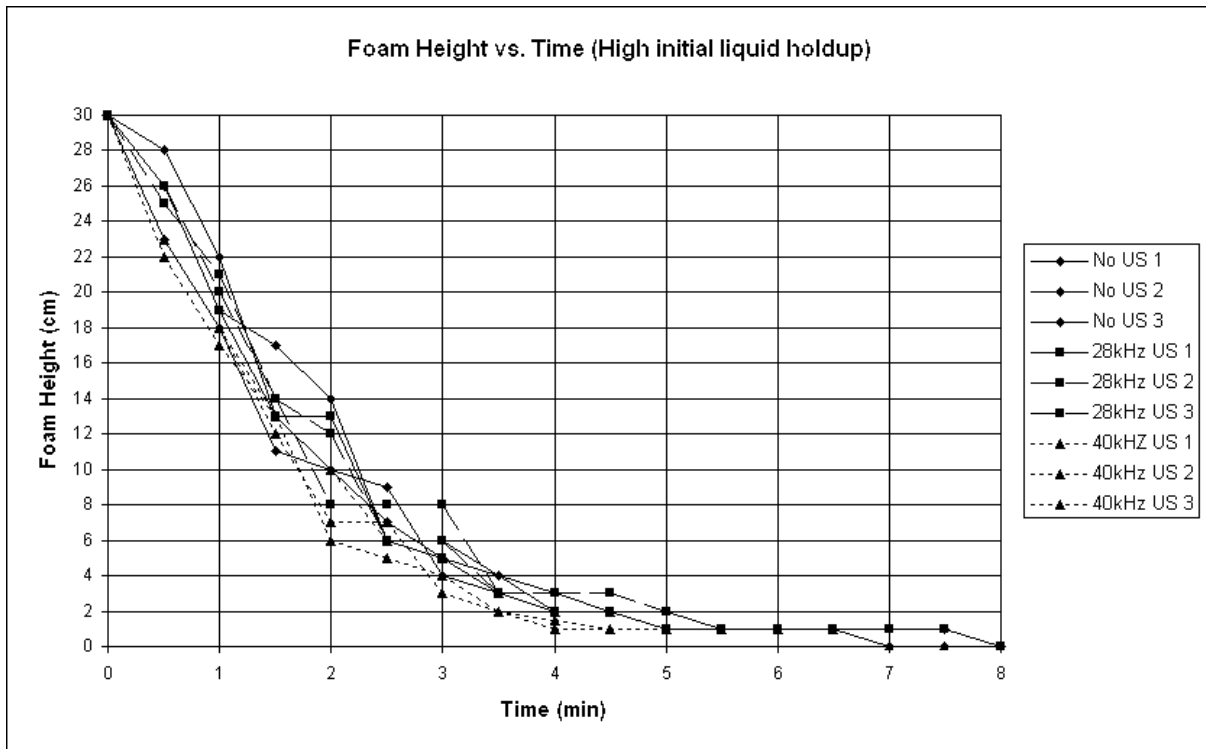


Fig 7.4.1-Raw foam height data for high initial liquid holdup.

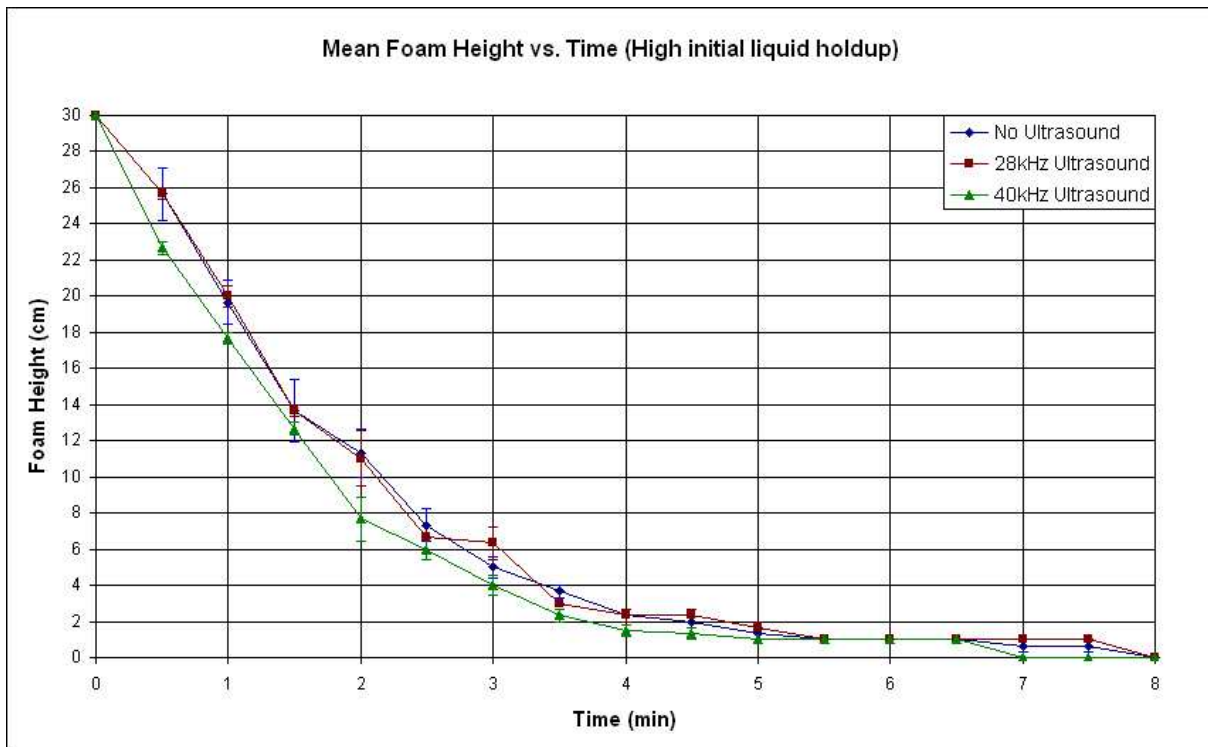


Fig 7.4.2-Averaged experimental variation of foam height with time for high initial liquid holdup.

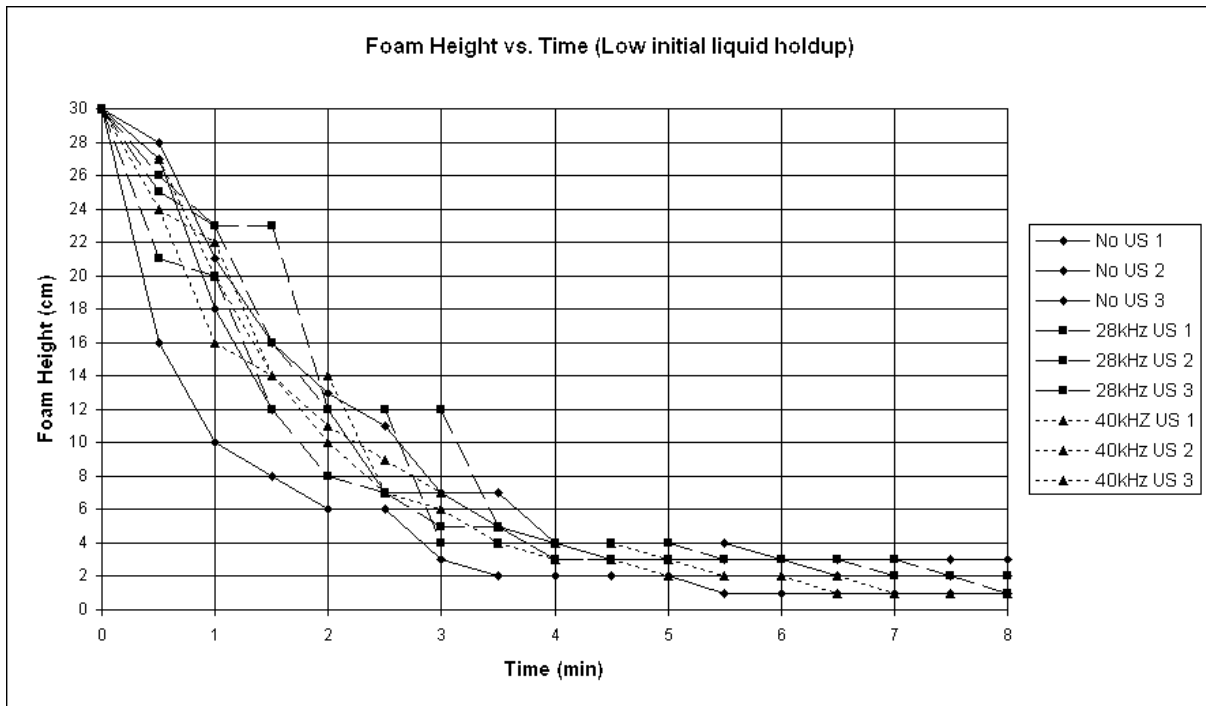


Fig 7.4.3-Raw foam height data for low initial liquid holdup.

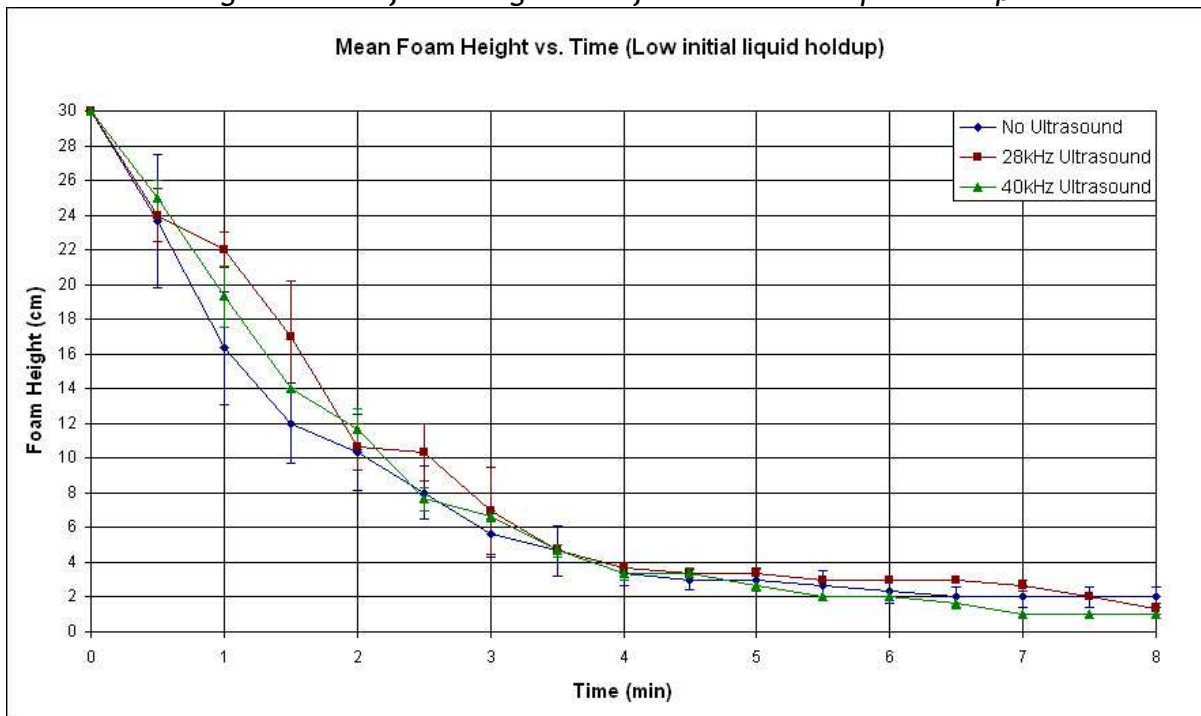


Fig 7.4.4-Average experimental variation of foam height with time for low initial liquid holdup.

7.5 Variation of mean liquid holdup during foam collapse:

Values of liquid holdup (ml liquid entrained/cm³ of foam) were computed from experimental cumulative liquid drainage and foam height data. As a consequence of this the value of liquid holdup at each time interval is a 'spatial' average, as no variation in liquid holdup with vertical position in the foam is accounted for. Initial liquid holdup values are averaged across the three experiments conducted at two different initial liquid holdups. Figure 7.5.1 shows a great variation in liquid holdup between foam subjected to no ultrasound and foam subjected to 40.00kHz ultrasound. In the case of the 40.00kHz ultrasound, low initial liquid holdup data mean liquid holdup increases by a factor of ≈ 2.3 . This significant increase in mean liquid holdup for both 40.00kHz plots is a result of local drainage characteristics of the foam and the rate of foam collapse (height reduction). The similar shapes of the two 40.00kHz ultrasound plots (one for each value of initial liquid holdup), both with peaks at $t=4$ minutes, indicate that the observed increase in mean liquid holdup is independent of the initial value of liquid holdup.

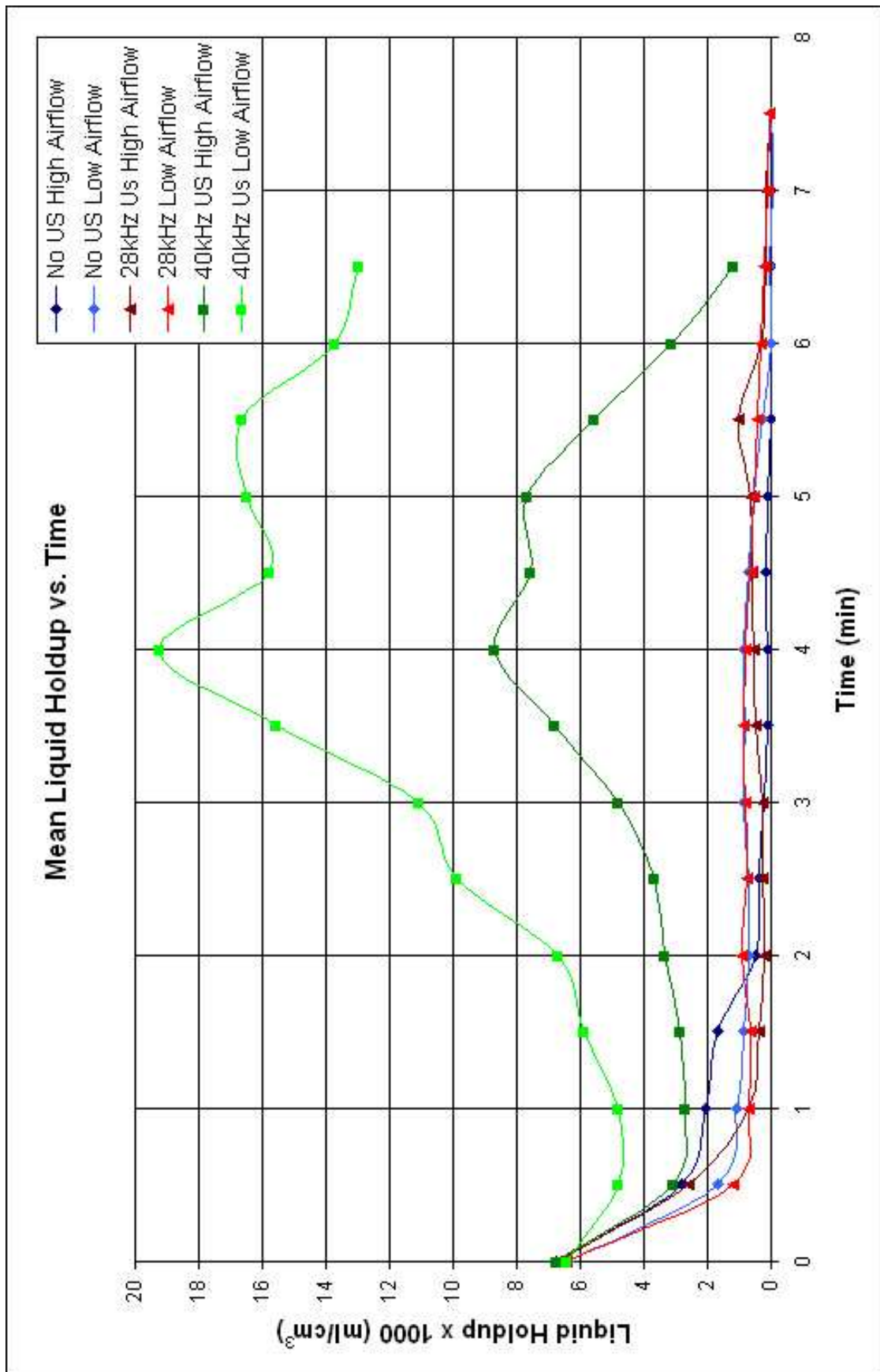


Fig 7.5.1-Experimental data showing the variation in mean liquid holdup with time.

7.6 Images of foam collapse:

The effects of foam drainage on lamellae thickness and foam collapse events were recorded with a high speed (250 frames/sec) Kodak EM camera on loan from the EPSRC. Figures 7.6.1 and 7.6.2 show the effect of liquid drainage on foam generated using 1 L/min airflow, subjected to no ultrasound and 40.00kHz ultrasound respectively. The images are 0.04 seconds apart (10 frames). From figures 7.6.1 and 7.6.2 it can be seen that 40.00kHz ultrasound causes increased thinning of lamellae, i.e. more liquid drainage occurs over the time period, compared to that which occurs in the absence of ultrasound.

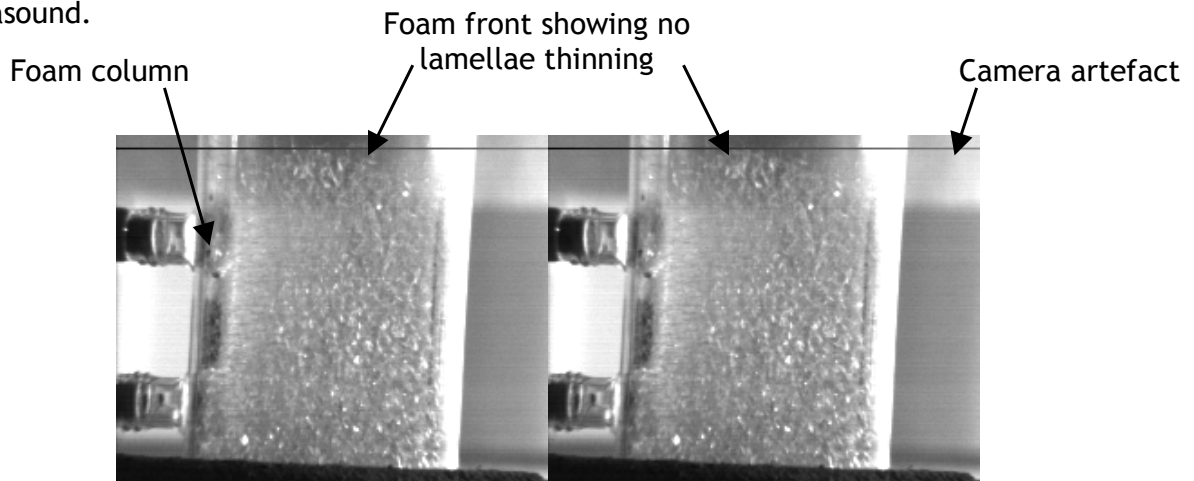


Fig 7.6.1-Liquid drainage of foam subjected to no ultrasound, 0.04 seconds between images.

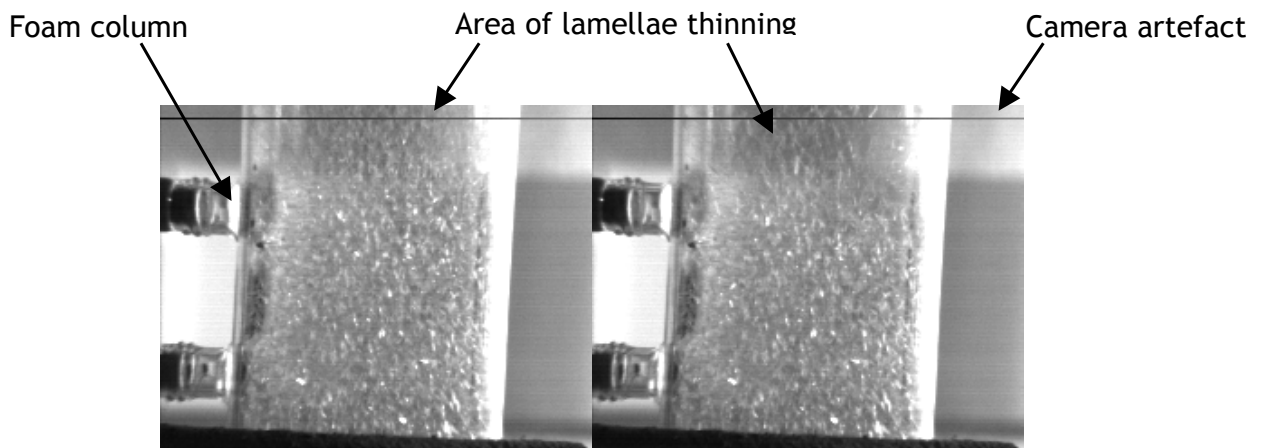


Fig 7.6.2-Liquid drainage of foam subjected to 40.00kHz ultrasound, 0.04 seconds between images.

Figure 7.6.3 shows images of foam collapse induced by 40.00kHz ultrasound. No such collapse events were observed in foam not subjected to ultrasound. Images are each 0.004 seconds (1 frame) apart. Collapse can be seen in the upper right section of the foam, a void being created after rupture.

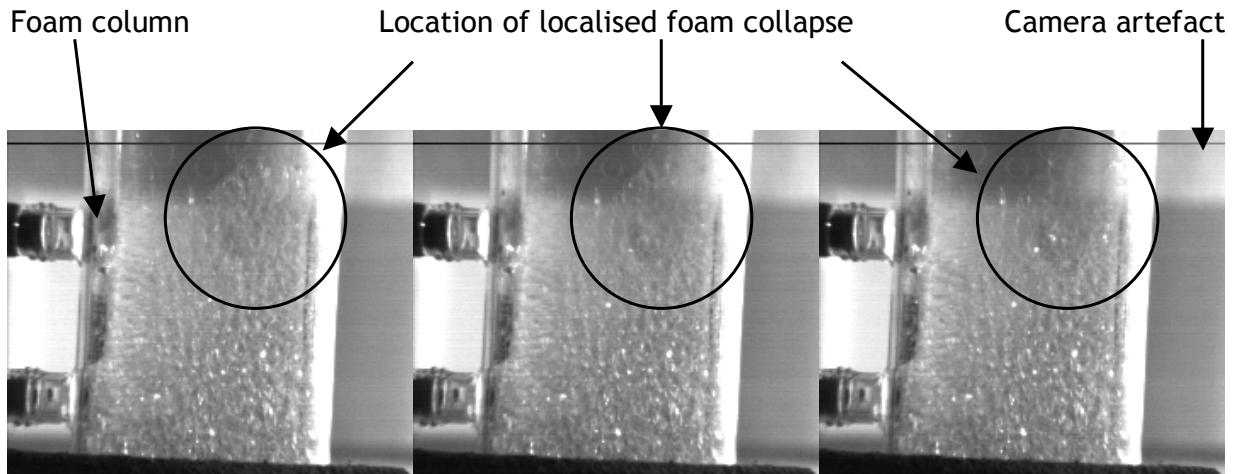


Fig 7.6.3-Collapse of foam subjected to 40.00kHz ultrasound, 0.004 seconds between images (rupture event lasts 0.012 seconds).

7.7. Foam fraction and ultrasonic foam breaker integration:

The ultrasonic transducer and plastic cup assembly was integrated with a fellow fourth year engineering science student's (David Wall, Mansfield College) foam fractionation experimental apparatus in an attempt to improve upon the foam breaking achieved with a mechanical rotating 'stirrer' arrangement. Efficient foam breaking is required by the foam fractionation process in order to collapse foam and provide an enriched solution for column reflux.

Figures 7.7.1 and 7.7.2 show photographs of the plastic cup and ultrasonic transducer assembly being utilised as a foam collector and breaker. The ultrasonic foam breaker was easily integrated with the foam fractionation column, but was ineffective at collapsing the foam, neither controlling the volume of foam in the plastic cup (which overflowed) or providing an adequate volume of liquid for reflux.

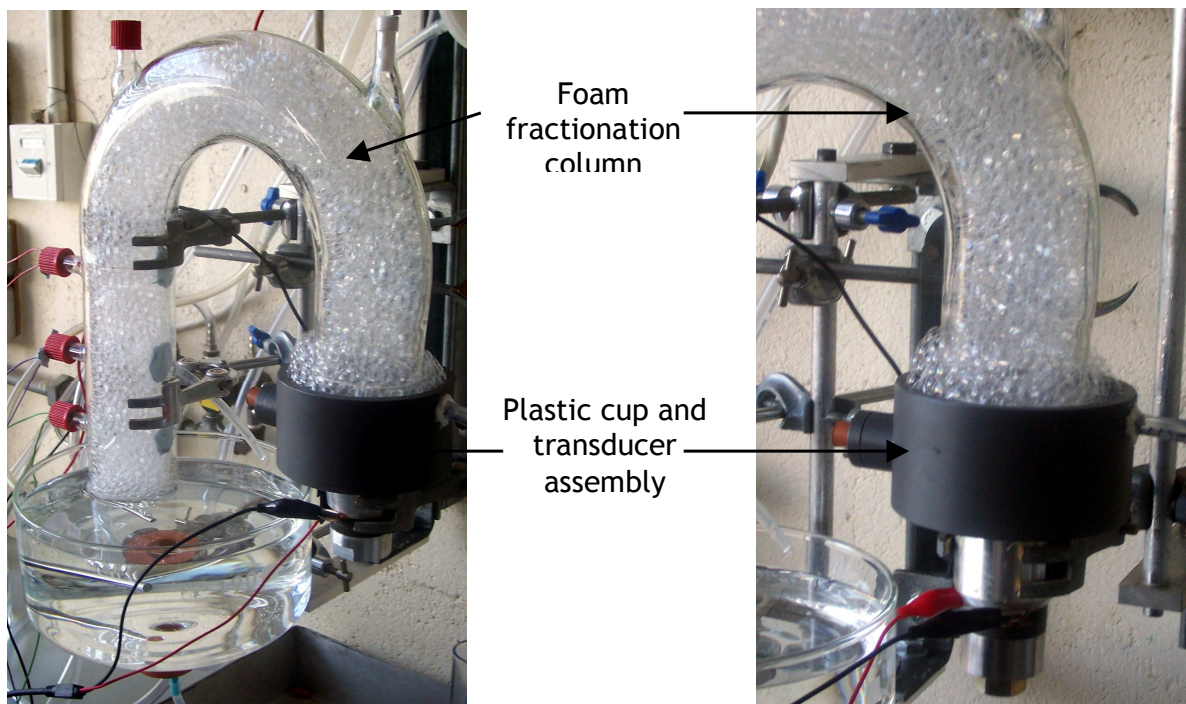


Fig 7.7.1- Foam fractionation and 40.00kHz ultrasound integration.

Fig 7.7.2- Foam fractionation and 27.72kHz ultrasound integration.

7.8 Experimental errors and reproducibility:

Taking figures 7.2.1 and 7.2.3 it is clear that significant offset errors exist in the cumulative liquid drainage data. These errors exist due to limitations of the experimental methodology used; difficulties arose in choosing the $t=0$ minutes datum. This datum was chosen manually using intuition rather than following a more systematic procedure. The general trends of the cumulative drainage plots are consistent between repeats however, so the offset error is eliminated in drainage rate plots (figures 7.3.1 to 7.3.6) by differentiation.

The fluctuations in the 40.00kHz liquid drainage rate shown in figures 7.3.5 and 7.3.6 are due to unexplained behaviour during one repeat of the experiment. As this repeat was carried out towards the end of the experimental run the author had built up enough experimental experience to notice the change in behaviour, but no obvious change in experimental conditions were found.

The increase and peak in the mean liquid holdup for foam of two different initial liquid holdups subjected to 40.00kHz ultrasound demonstrates that experimental results are repeatable. The existence of similar characteristics in two completely separate sets of data also gives increased confidence in the validity of results obtained.

8. Discussion of Results:

8.1 Rate of liquid drainage and cumulative global drainage:

The general increase in liquid drainage rate shown in figures 7.3.2, 7.3.3, 7.3.5 and 7.3.6, obtained from directly measuring the cumulative mass of liquid drainage is confirmed visually by the images showing increased thinning of lamellae in a foam exposed to 40.00kHz ultrasound, see figure 7.6.2. The consequence of the increased liquid drainage rate is an increase in foam collapse rate, as demonstrated by foam height results. These observations experimentally confirm the proposals made by Sandor and Stein (1993) that ultrasound causes accelerated film drainage, leading to lamellae reaching their critical thickness in a shorter time period, hence increasing the foam collapse rate. It is also apparent from figure 7.6.3 that 40.00kHz ultrasound affects the manner in which foam collapse occurs. One critical parameter that has not been measured experimentally is lamellae thickness. Whilst liquid drainage and foam height results confirm the existence of a threshold lamellae thickness, which is expected from characterisations of the experimentally observed front rupture mechanism encountered in the literature review, it has not been determined if 40.00kHz ultrasound actually alters the threshold thickness or whether it is purely a function of foam rheology. A frequency dependence is noted, similar observations were not made with 27.72kHz ultrasound, which had no measurable effect on liquid drainage rate.

Considering the plots of cumulative liquid drainage, as shown in figures 7.2.2 and 7.2.4, it seems that the significantly lower quantity of initial global liquid drainage in the case of 40.00kHz ultrasound indicates that the threshold lamellae thickness is indeed increased. However, the significant increase and peak in mean liquid holdup, shown in figure 7.5.1, must also be considered. It is entirely possible that local drainage at the rupture front of the foam is significantly increased, while the increase in mean liquid holdup results in reduced global liquid drainage. To understand this requires measurements of local liquid drainage from foam, a variable that was not measured experimentally in this study.

8.2 Mean liquid holdup:

The most prominent feature of the variation of mean liquid holdup with time, see figure 7.5.1, is the peak occurring after four minutes of drainage, enhanced by 40.00kHz ultrasound, have elapsed. The similar results for both initial liquid holdups demonstrate that the peak in mean liquid holdup is itself not a function of initial liquid holdup. The observed peak in mean liquid holdup confirms that entrained liquid released by a rupture event is first taken up by the surrounding plateau borders, rather than directly draining into the bulk of the surfactant solution. The increased rate of bubble rupture, stimulated by 40.00kHz ultrasound, leads to the rise and peak in liquid holdup. Immediately after rupture there is a larger proportion of liquid still entrained in a reduced volume of foam, these conditions giving rise to the peak in average liquid holdup. One other factor to consider is the quantity of liquid that plateau borders can take up, a function of liquid holdup itself. The subsequent decrease in mean liquid holdup after the peak at 4 minutes is probably due to there being an insufficient volume of foam remaining to take up the liquid released by bubble rupture, this excess liquid instead draining straight into the bulk of the surfactant solution. Evidence for this can be seen in plots of foam height and the rise in liquid drainage rates observed for 40.00kHz ultrasound after 4 minutes have elapsed, figures 7.3.3, 7.3.6, 7.4.2 and 7.4.4.

8.3 Foam Collapse:

The experimentally observed increase in liquid drainage from foam subjected to 40.00kHz ultrasound is consistent with the expected mode of foam rupture, front rupture, as described in section 5.2. Further understanding of the mechanics of foam collapse requires consideration of simplified drainage and foam collapse scenarios and comparison to a plot of experimental data showing foam height against cumulative liquid drained, figures 8.3.1 (high initial liquid holdup) and 8.3.2 (low initial liquid holdup).

Figure 8.3.3 shows the same foam height and volume of liquid drained relationship as figures 8.3.1 and 8.3.2 for three simplified foam height and liquid holdup scenarios. Curve 1 shows the idealised relationship between foam height and volume of liquid drained for a foam in which no film rupture occurs, whilst liquid drainage proceeds at a constant rate i.e. liquid holdup reduces with time. Curve 2 corresponds to random bubble coalescence throughout the foam, with a constant total gas volume and liquid holdup. Finally, curve 3 refers to foam undergoing collapse, with a rupture front at the top surface, whilst no liquid drainage occurs; hence liquid holdup increases as foam rupture progresses.

Comparison of figures 8.3.1, 8.3.2 and 8.3.3 allows for the dominant collapse regime of the foams used in experimental work to be identified. From the shape of the 40.00kHz ultrasound curve in figure 8.3.1 it is apparent that initially front rupture dominates, with little global drainage occurring. As global drainage progresses the rate of liquid drainage increases until a point is reached at which very little film rupture occurs. In the case of 27.72kHz ultrasound and no ultrasound random coalescence of the foam causes a significant amount of foam collapse. This was noted by the absence of large rupture events at the top surface of the foam such as those shown in figure 7.6.3 for 40.00kHz ultrasound. The flat plateau for $t > 6$ minutes seen for 40.00kHz ultrasound in figure 8.3.2 suggests that at this point little foam collapse is occurring whilst drainage progresses. This is consistent with the reduction in mean liquid holdup over this period, see figure 7.5.1. Whilst the apparent lack of bubble rupture ties in with experimental observations of foam persistence due to surfactant enrichment in the case of foam generated at the lower, 0.5 L/min, airflow rate.

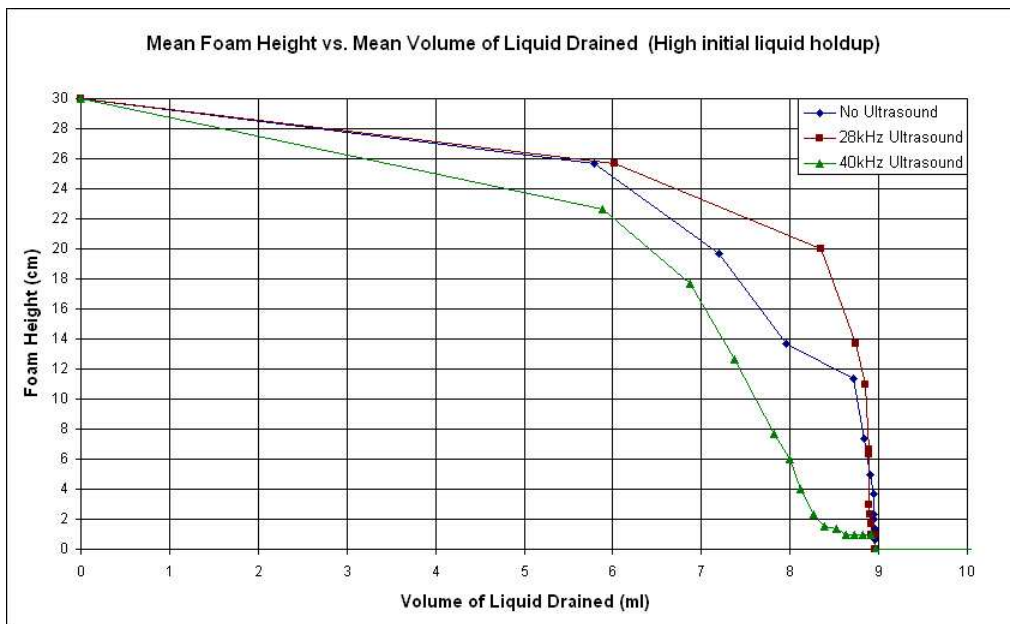


Fig 8.3.1-Foam height vs. volume of liquid drained. High initial liquid holdup.

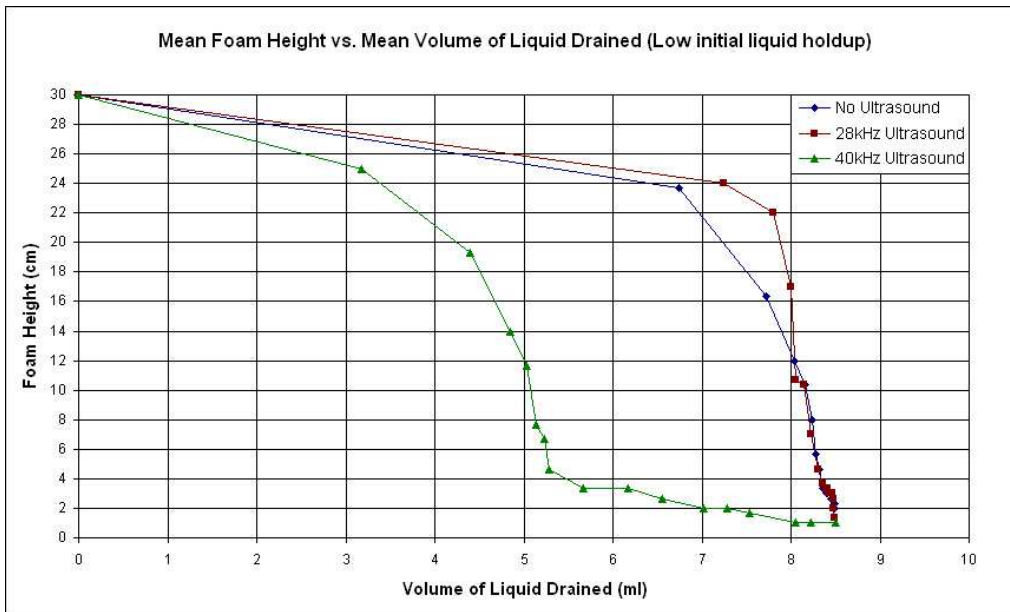


Fig 8.3.2-Foam height vs. volume of liquid drained. Low initial liquid holdup.

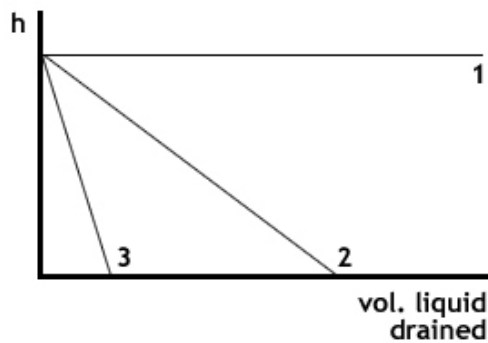


Fig 8.3.3-Foam height and volume of liquid drained curves for three simplified drainage scenarios.

9. Project Extensions:

The most significant hurdle to further understanding of foam-ultrasound interaction is quantifying the actual acoustic energy transferred to the foam by the ultrasonic transducer. Overcoming this problem would allow conclusions to be drawn regarding the amplitude of vibrations required to rupture lamellae. Measuring the ultrasonic pressure field in the presence of foam would be the first step towards the solution.

Progression of experimental work requires the design of apparatus that allows for higher voltages to be used safely (voltage was limited to 50v in this study by safety constraints) so that the ultrasonic transducers can be supplied with more electrical power. The new design must isolate the ultrasonic transducer from the foam to avoid any water-liquid contact, whilst not creating any large impedance boundaries to reflect the ultrasound and hinder coupling to the foam. Increasing the range of electrical power available would allow for investigation of the relationship between power supplied to the transducer and foam collapse rate.

In depth knowledge of the effect of ultrasound on local foam drainage is required, direct measurement of the variation in local liquid holdup with time, using either a foam sampling method or electrical resistance tomography (which measures changes in conductivity as lamellae drain and thin), would provide this understanding. Both methods have drawbacks however, notably foam sampling is intrusive and would disrupt the foam, but could still be employed to indicate where the liquid holdup peak occurs. Further investigation into the spatial variation of liquid drainage could also be related to the acoustic pressure field.

In tandem with refinement of experimental procedures developing a model of foam destruction by ultrasound would be beneficial. No such models currently exist; modelling work would have to draw upon single film drainage models, the first step being describing drainage under the influence of gravity (drainage equation) and ultrasound of an idealised ordered foam. Linking this with existing research concerning acoustic levitation of single bubbles and their normal modes of vibration (McDaniel and Holt, 2000). It is envisaged that constructing a successful model would also require more detailed experimental work on ordered 'bespoke' foams to increase the understanding of bubble resonance.

10. Conclusions:

This project has demonstrated, for the first time at the University of Oxford's Department of Engineering Science, that ultrasound can be effectively employed to increase the collapse rate of detergent based foams. Application of knowledge gained from undertaking a comprehensive literature review to designing the experimental apparatus allowed for effective transmission of ultrasound to the foam, resulting in a higher foam collapse rate being achieved at an average electrical power of 4 W (supplied to the ultrasonic transducer); lower than any previous research encountered in the literature.

Experimental results illustrate that ultrasound increases the rate of liquid drainage from foam, and hence increases the foam's collapse rate. This corroborates the observations of Sandor and Stein (1993). The dominance of the front rupture collapse mechanism, which is itself characterised by a threshold lamellae thickness, confirms that the presence of ultrasound causes lamellae to reach critical thickness quicker than in its absence. However it is not apparent if ultrasound also initiates lamellae rupture at a greater critical thickness as this parameter was not measured. It has also been shown that similar effects and trends are observable for two different values of initial liquid holdup. All experimental data obtained show that 40.00kHz ultrasound has significantly more pronounced effects than 27.72kHz ultrasound. It is likely that at higher powers this frequency dependence may change, although further work is required to confirm this as fact.

From analysing liquid drainage and foam height data the relationship between average liquid holdup throughout the foam and time was obtained. It is evident that 40.00kHz ultrasound causes a large increase in average liquid holdup. This confirms that liquid released by a rupture event is first taken up by the surrounding plateau borders, rather than directly draining into the bulk of the surfactant solution. In the case of 40.00kHz ultrasound it was observed that foam collapse occurs at lower values of global drainage than in the absence of ultrasound, meaning that immediately after rupture there is a larger proportion of liquid still entrained in a smaller volume of foam than compared to foam subjected to 27.72kHz ultrasound/no ultrasound. This coherent combination of conditions gives rise to the peak in average liquid holdup. It is expected, due to the front rupture mechanism, that the increase in liquid holdup is sharpest at the top of the

foam, i.e. at the rupture front. Direct measurements of local liquid holdup would give a more detailed understanding of the variation of local liquid holdup throughout the foam.

The plastic cup assembly was integrated with a fellow fourth year engineering science student's (David Wall, Mansfield College) foam fractionation experimental apparatus in an attempt to improve upon the foam breaking achieved with a mechanical rotating 'stirrer' arrangement. It was found that the ultrasound was ineffective at controlling the foam. More experiments are required at a higher electrical power to confirm whether ultrasound can be successfully used in this application.

Appendix:

A. Progress Report:

A.1 Description of project:

The main focus of this project is to investigate the effect of ultrasound (20kHz and above) on the stability of foams. In industrial applications, such as fermentation, the destruction of unwanted foams is often difficult and achieved either by mechanical or chemical means, both involving contact and the potential for product contamination. Ultrasound offers a 'clean' foam breaking method without the need for intimate contact between the ultrasonic transducer and foam.

Alongside knowledge of the physics of foams themselves, information is required on the generation of ultrasound- transducers and piezoelectric materials. The effective transmission of ultrasound from air into foam requires attention (due to the large impedance discontinuity).

A.2 Tasks identified:

- Literature review to gain an understanding of basic concepts of foam stability, drainage and collapse. An appreciation of past experimental procedures and research is required.
- Key parameters need to be decided on. Possible variables include: Ultrasound amplitude, ultrasound frequency, transducer geometry, surfactant type, and bubble diameter.
- Design of a series of experiments to investigate foam stability, based upon the variables identified. Aim to verify information gained from literature review and gain an insight into ultrasound/foam contacting. Order equipment needed. Photograph/document experiments for use in project report.
- Carry out experimental work and data collection.
- Analysis of results, leading to more experimental work if necessary.
- Modelling of foam/ultrasound interaction and subsequent collapse.

A.3 Results achieved so far:

So far the majority of time has been spent reading papers on the subject to form a background of understanding as a basis of the project and on refining experimental technique. Due to this only one set of meaningful results has been obtained see figure A.3.1.

These results are from measuring liquid drainage with time from foam created in an ultrasonic bath (ultrasound generated at 25kHz). Whilst repetition is needed to make judgements with regard to errors, it can be said that the effect of ultrasound is to increase the rate of liquid drainage from the lamellae within the foam structure. This agrees with the mechanism for foam destruction proposed in the literature whereby foam destruction occurs due to increased drainage, and hence enhanced film thinning, leading to films attaining their critical thickness over a shorter time period.

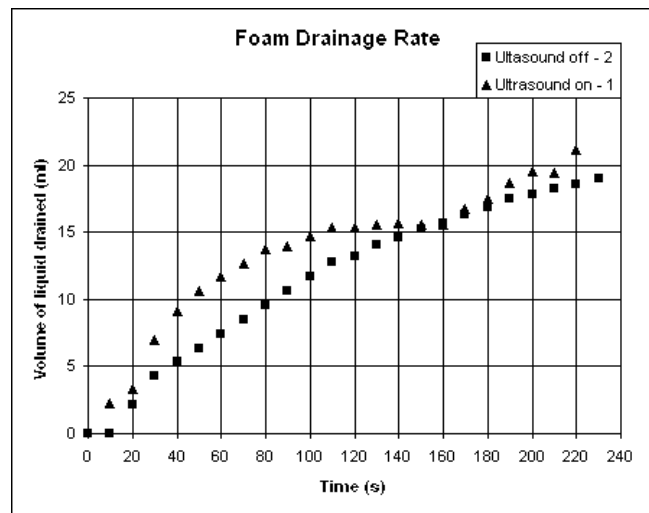


Fig A.3.1-Initial foam drainage results.

A.4 Problems:

The biggest challenges to the success of this project are; the generation of relatively uniform 'bespoke' foams (narrow bubble size distribution) and also accurately measuring this parameter. This problem is being worked around by practising experimental technique and applying knowledge gained from background reading. Another difficulty lies in ensuring sufficient energy is transmitted from the ultrasound to the foam. So far

no practical steps have been taken in this regard, but knowledge of impedance boundaries is being revised (2nd year PDE's course).

A.5 Future work:

Week 7,8 MT: Completion of preliminary experiments and design of final experimental setup

Winter break: Write literature review section for project report and characterise transducers obtained

Week 1,2 HT: Obtain any further equipment needed for experimental rig and make final decision on experiments to be conducted

Week 3,4 HT: Begin conducting experiments

Week 5,6 HT: Aim to complete data collection

Week 7,8 HT: Analysis of results

Spring Break: Complete outstanding experimental work and write project report

Week 1,2 TT: Finish writing report and submit draft to project supervisor

Week 3,4 TT: Submit report to examiners

B. Plastic Cup Design:

Figure B.1 shows the design of the plastic cup arrangement used in experimental work.

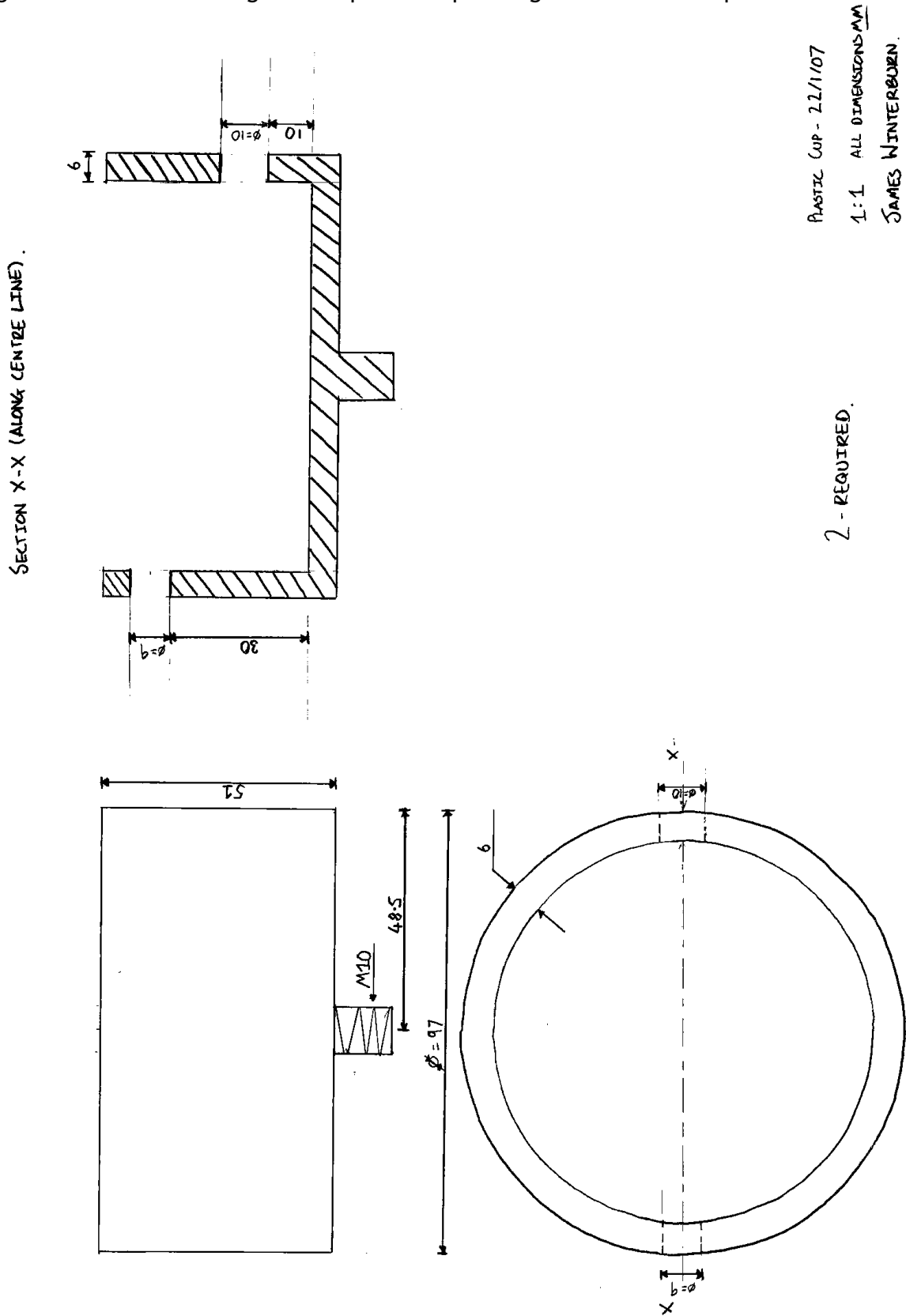


Fig B.1-Plastic cup design drawing.

C. Ultrasonic Transducer Pressure Calibrations:

Figures C.1 to C.6 show the absolute, axial and transverse pressure calibrations for the 27.72kHz and 40.00kHz transducers. With thanks to Jamie Condliffe.

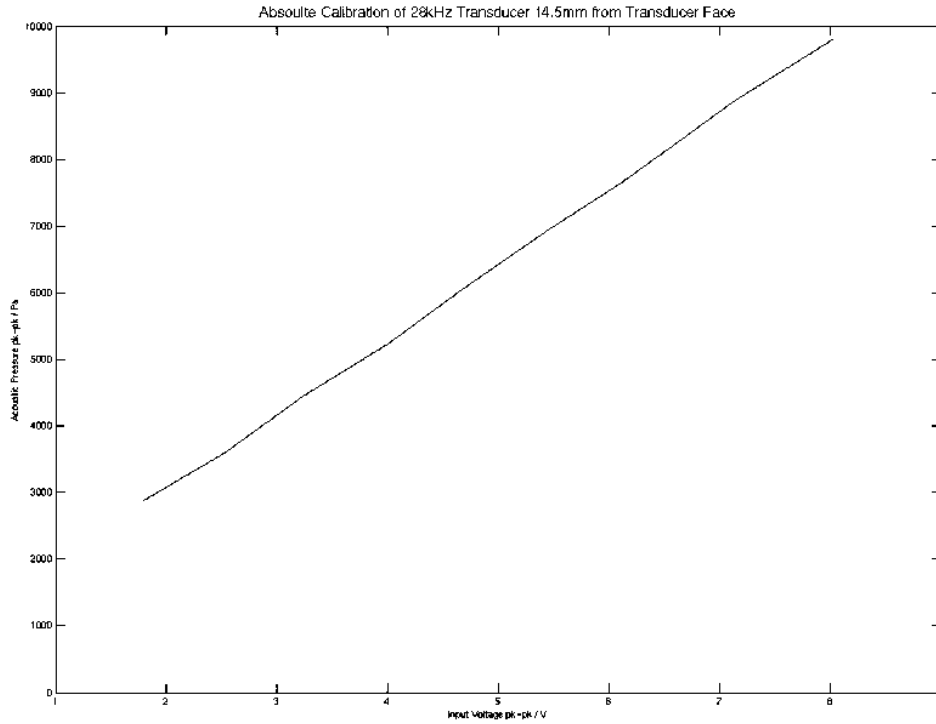


Fig C.1- 27.72kHz transducer absolute pressure calibration.

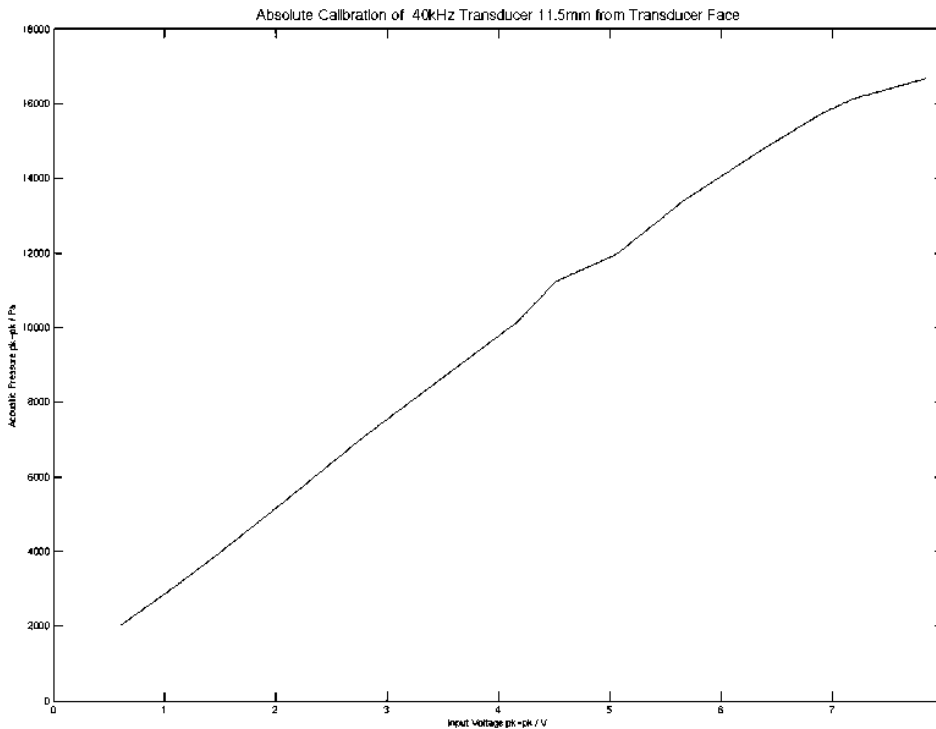


Fig C.2- 40.00kHz transducer absolute pressure calibration.

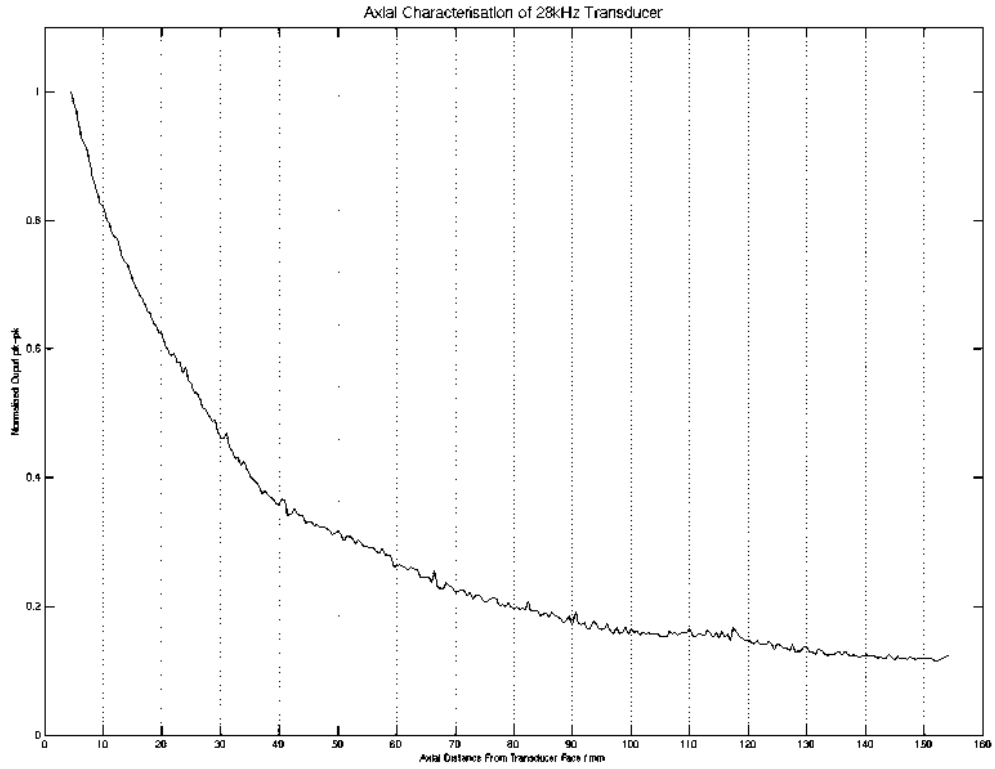


Fig C.3-27.72kHz transducer axial calibration.

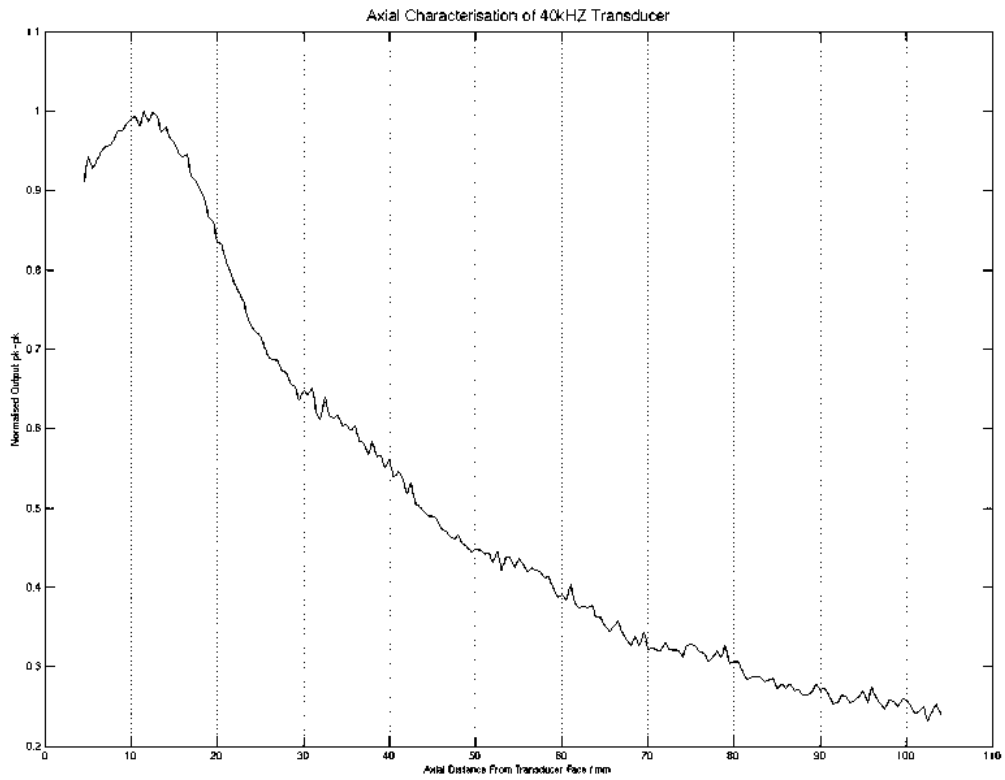


Fig C.4-40.00kHz transducer axial calibration.

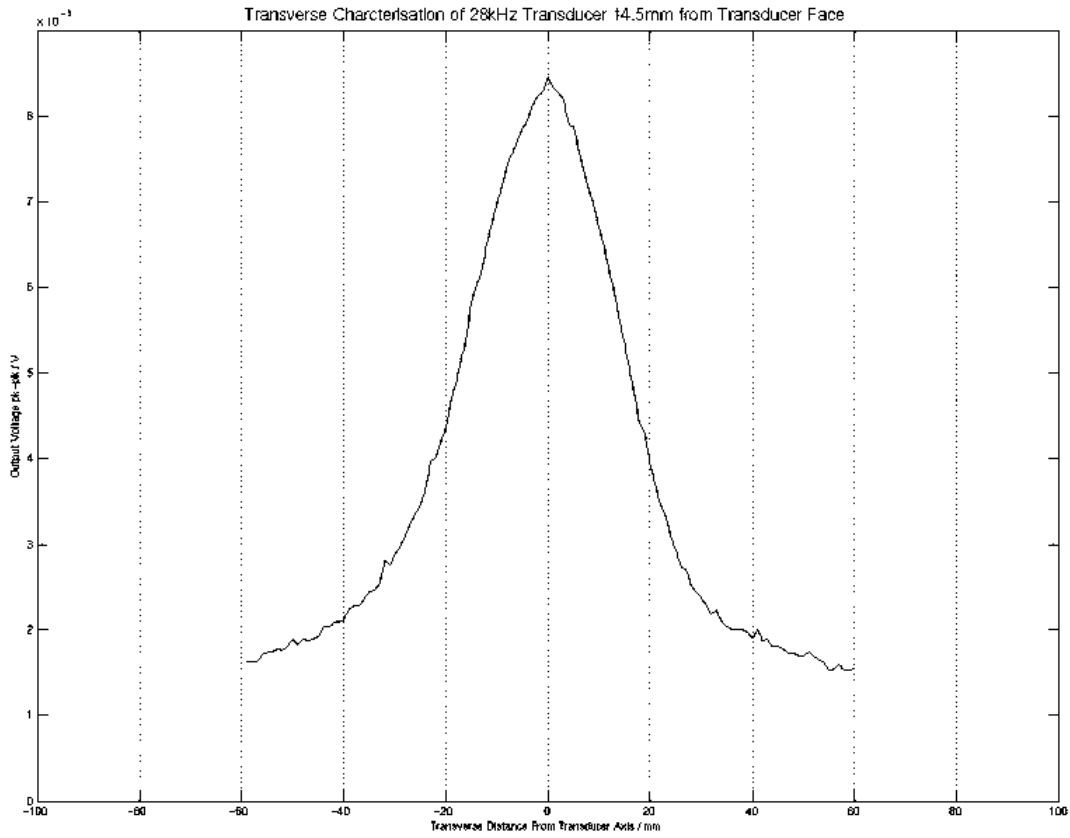


Fig C.5-27.72kHz transducer transverse calibration.

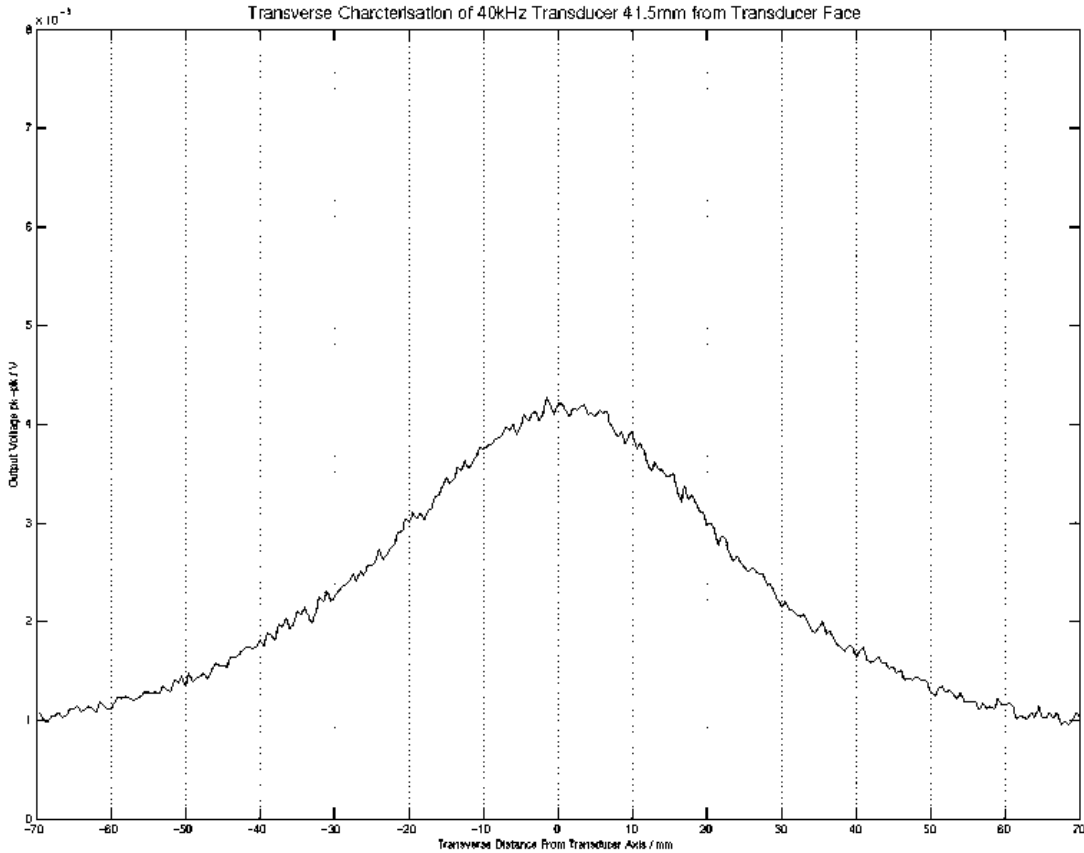


Fig C.6-40.00kHz transducer transverse calibration.

D. Preliminary Results

Figure D.1 contains results from preliminary ultrasonic bath experiments.

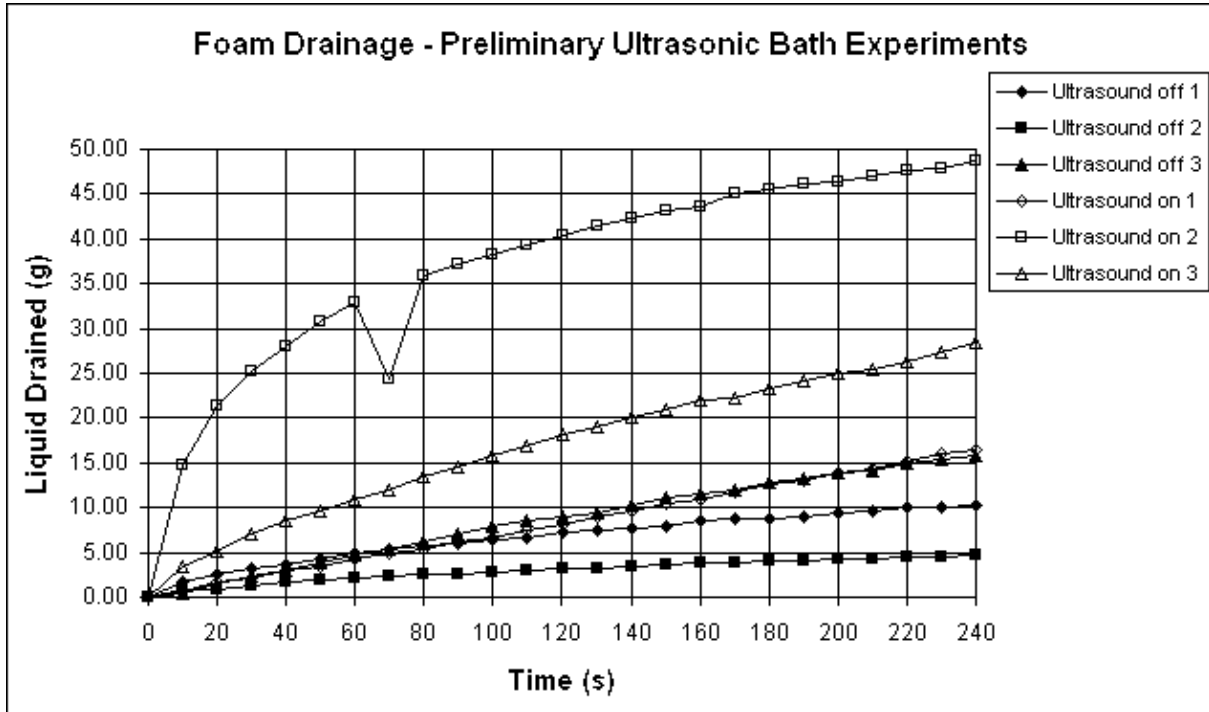


Fig D.1-Foam drainage data obtained from preliminary ultrasonic bath experiments. 25kHz ultrasound.

E. Risk Assessment:

4th Year Project Risk Assessment

Department of Eng Science

Form RA01 16/10/03

Risk Assessment		4YP - Sound Methods of Breaking Foam		Page 1 of 1	
In Building		Thom Building, 3 rd Floor, room 3.02B			
Assessment undertaken		James Winterburn		Signed <i>J. Winterburn</i> Date: 31/10/06	
Assessment supervisor		Peter Martin		Signed <i>P. M.</i> Date: 31/10/06	
Hazard	Persons at Risk	Risk Controls In Place	Further Action Necessary To Control Risk		
Compressed Air.	Myself.	Pressure regulator fitted to air supply line. Riser is not pressure tested, inspect for blockages before each use.	Check PAT test label is still valid and contact electronics department if re-test is due.		
240 V AC Electric shock.	Myself.	Ensure all electrical equipment is PAT tested.			
Water & electricity.	Myself and others in the lab.	Fail-safe circuit breakers fitted to electrical distribution system. Care is to be taken that no plugs, leads etc. are placed in areas where water can accumulate.			
Ultrasonic Bath.	Myself.	Operate only in accordance to manufacturers instructions. Bath should be at least ¾ full of liquid when in use.			
Glassware.	Myself and others in the lab.	All glassware should be handled with care. Any breakages should be dealt with immediately and broken glass disposed of in the appropriate manner.			
Domestic Surfactant (CPC).	Myself.	Irritant- see COSHH assessment.			
Triton-X-100 Surfactant	Myself.	Harmful- see COSHH assessment.			
Teepol Detergent	Myself.	Irritant- see COSHH assessment.			

Your E-mail Address: james.winterburn@pmb.ox.ac.uk

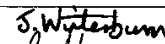
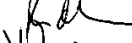

Checked by *(DJ Reed)*

Date: 31/10/06

UPS S2/97

F. COSHH Assessment:

COSHH Assessment Form

<i>If insufficient space is available under any section, use a separate piece of paper and attach it to the form.</i>		Serial No:			
		Date: 30 th October 2006			
Department: Engineering Location of work: Thom Building, 3 rd Floor, room 3.02B		Persons involved: James Winterburn.			
Description of procedure: <p style="text-align: center;">Use of surfactants for the generation of foams.</p>					
Substances used:		Quantities Used	Frequency of use	Hazards identified	Exposure route
Triton-X-100. Teepol Detergent. Domestic surfactant (CPC).		Variable but small. Typically in range 0.1-2.0 wt% (In solution with water).	2-3 days per week.	Harmful. Irritant. Irritant.	Eyes and skin- most likely via hands from handling substance.
Could a less hazardous substance (or form of substance) be used instead? No Justify not using it:					
What measures have you taken to control risk? Engineering controls: N/A PPE: Wear eye protection. Lab coats to be worn. Use disposable gloves and replace frequently if using large quantities to avoid the possibility of skin contact. Management measures: Persons susceptible to allergic reactions should not work with these materials.					
Checks on control measures: N/A					
Is health surveillance required? No		Training requirements: To be aware of the need for good personal hygiene, potential for and symptoms of skin sensitisation.			
Emergency procedures: Fire: CO2, Dry powder, Foam. Spillage: Mix with inert material and place in suitable containers for disposal.		Waste disposal: Non-hazardous.			
Name and position of assessor: James Winterburn		Signature: 			
Name of supervisor (student work only): Dr Peter Martin		Signature: 			
Name of head of department or nominee (DSO): D J Reed (DSO)		Signature: 			

1/10/06

G. References:

Barigou, M. and Davidson, J.F. (1994) Soap film drainage: theory and experiment. *Chemical Engineering Science*. **49**(11), 1807-1819.

Blitz, J. (1956) *Ultrasonics-Methods and Applications*. 8th Edition. Butterworths.

Brady, M. (2004) 2nd year PDE lecture notes.

Coons, J.E., Halley, P.J., McGlasham, S.A. and Tran-Cong, T. (2005) Scaling laws for the critical rupture thickness of common thin films. *Colloids and Surfaces A: Physicochem. Eng. Aspects*. **263**, 258-266.

Dedhia, A.C., Ambulgekar P.V. and Pandit, A.B. (2004) Static foam destruction: Role of ultrasound. *Ultrasonics Sonochemistry* **11**(2), 67-75.

Dexter, A.F., Malcolm, A.S. and Middleberg. A.P.J (2006) Reversible active switching of the mechanical properties of a peptide film at the fluid-fluid interface. *Nature Materials*. Advance online publication 21st May.

Ensminger, D. and Dekler, M. (1973) *Ultrasonics- Low and High-Intensity Applications*.

Gutwald, S. and Mersmann, A. (1997) Mechanical foam breaking- a physical model for impact effects with high speed rotors. *Chem. Eng. Technol.* **20**, 76-84.

Heller, J.P. and Kuntamukkula, M.S. (1987) Critical review of the foam rheology literature. *Ind. Eng. Chem. Res.* **26**, 318-325.

Howard, D.M. and Angus, J. (2006) *Acoustics and Psychoacoustics*. 3rd Edition. Focal Press.

Howatson, Lund and Todd (HLT) (1991) *Engineering Tables and Data*, Chapman and Hall.

Kralchevsky, P., Danov, K. and Denkov, N. (2002) Chemical Physics of Colloid Systems and Interfaces. *Extract from Handbook of Surface and Colloid Chemistry*. 2nd Edition. CRC Press.

Kukarni, R.D., Goddard, E.D. and Kanner, B. (1977) Mechanism of antifoaming: role of filler particle. *Ind. Eng. Chem., Fundam.* **16**(4), 472.

Lim, K.S. and Barigou, M. (2005) Ultrasound-assisted generation of foam. *Ind. Eng. Chem. Res.* **44**, 3312-3320.

Marze, S.P.L., Saint-Jalmes, A. and Langevin, D. (2005) Protein and surfactant foams: linear rheology and dilatancy effect. *Colloids and Surfaces A: Physicochem. Eng. Aspects* **263** 121-128.

McDaniel, J.G. and Holt, R.G. (2000) Measurement of aqueous foam rheology by acoustic levitation. *Rapid Communications-Physical Review E* **61**(3).

McKenzie Smith, I. *et al.* (2002) Hughes Electrical and Electronic Technology. 8th Edition. Pearson.

Monin, D., Espert, A. and Colin, A. (2000) A new analysis of foam coalescence: from isolated films to three-dimensional foams. *Langmuir* **16** 3873-3883.

Morey, M.D., Deshpande, N.S. and Barigou, M. (1999) Foam destabilization by mechanical and ultrasonic vibrations. *Journal of Colloid and Interface Science* **219**, 90-98.

Narsimhan, G. and Wang, Z. (2006) Rupture of equilibrium foam films due to random thermal and mechanical perturbations. *Colloids and Surfaces A: Physicochem. Eng. Aspects* **282-283**, 24-36.

Perry, R.H. and Green, D. (1984) Perry's Chemical Engineers' Handbook. 6th Edition. McGraw-Hill.

Reira, E., Gallego-Juárez, J.A. and Mason, T.J. (2006) Airborne ultrasound for the precipitation of smokes and powders and the destruction of foams. *Ultrasonics Sonochemistry* **13**(2),107-116.

Sandor, N. and Stein, H.N. (1993) Foam destruction by ultrasonic vibrations. *Journal of Colloid and Interface Science* **161**, 265-267.

Takesono, S., Onodera, M., Yoshida, M. and Yamagiwa, K. (2002) Performance characteristics of mechanical foam breakers fitted to a stirred-tank reactor. *Journal of Chemical Technology and Biotechnology*. **78**, 48-55. (2002).

Weaire, D. and S.Hutzler, S. (1999) *The Physics of Foams*. Oxford University Press.

Wedlock, D.J. *et al.* (1994) *Controlled Particle, Droplet and Bubble Formation*. Butterworth Heinemann.

http://www.channelindustries.com/chan_cat.pdf. (1999) Piezoelectric Ceramics. Channel Industries Inc. Accessed 9/10/06

www.morganelectroceramics.com. Sensors and Transducers. Morgan ElectroCeramics. Accessed 9/10/06

<http://www.grasp.ulg.ac.be/research/foam/>

Technical Notes. Given by supervisor Dr P.Martin